Computations of the Growth by Condensation of a Population of Cloud Droplets

By W. MORDY, International Meteorological Institute in Stockholm[1]

(Manuscript received June 15, 1958)

Abstract

The number and size of cloud droplets formed on several condensation nucleus spectra is computed numerically. The relative humidity is treated as a dependent variable and the settling of droplets by Stokes Law is accounted for.

A model is presented for studying simultaneous variations in vertical velocity, nucleus distribution, and humidity by the use of an electronic computer. To date eight computations have been made for three types of nucleus spectra at different rates of rise. Both nucleus distribution and rate of rise produce significant differences in resulting cloud droplet distributions.

The concentration of cloud droplets computed ranges from 1 cm^{-3} to 470 cm^{-3} for vertical velocities ranging from 5 cm/sec to 100 cm/sec.

1. Introduction

In the development of a cloud the spectrum of droplet sizes is initially determined by the number and size of condensation nuclei and the rate of cooling of the air. Subsequently the spectrum is altered by turbulence, coalescence, evaporation, sedimentation, and entrainment or mixing. Still later modification may occur by the Bergeron process.

Because these later processes act to modify the *initial* distribution it is important in the study of such processes to know in some detail the character and importance of the factors which control the shape of this *initial* distribution formed by condensation.

To date one of the most complete investigations of this kind has been made by HOWELL (1949) who investigated the growth of a population of varied sized droplets in air cooled at a uniform rate. In the years following Howell's work Woodcock made detailed measurements of the number and size of condensation nuclei larger than 10^{-12} g (Howell's max. size) and found them to be a very important portion of the nucleus spectrum in terms of the mass of salt found in the air.

The spectra of condensation nuclei used by Howell therefore will be replaced here by new ones based on more recent information which indicates appreciable numbers of very large nuclei. These "giant nuclei", as they are sometimes called, are in some instances large enough at cloud base to have appreciable fall velocities, a factor for which it was not necessary to account in Howell's investigation. A new investigation requires therefore also that this sedimentation of droplets be considered.

Howell formulated a growth equation for a droplet growing by condensation. It is an ordinary differential equation in which the growth is mainly dependent on only four

[1] This work has been supported by the U.S. Office of Naval Research and the Woods Hole Oceanographic Institution. Contribution number 1028 of the Woods Hole Oceanographic Institution.

factors, namely the radius, humidity, nucleus size, and time. Because of the very large variations in the growth rate of different sized condensation nuclei, and because of the "feed back" of the water vapor consumption, by condensation, on the humidity of the droplet environment, integration of this equation for a population of droplets becomes a laborious task. Howell proceeded with hand computations for three cases, believed to be characteristic of natural conditions and chosen to represent conditions which would demonstrate variations in the drop size spectrum. He found among other conclusions that the "conditions under which operation of the growth equation most favors a broad spectrum are not adequately clarified". This somewhat indecisive result was due at least partly to inadequate information about the condensation nuclei.

With modern computer techniques and with new observational information it now seems desirable to make a new and extended approach to this problem.

The author presents here a mathematical model which lends itself to an extension of Howell's work by investigation of a number of additional factors which influence droplet growth by condensation.

2. The model and its behavior

Consider a column of air rising vertically. At the base of this column, air is being introduced which contains a given population of different sized condensation nuclei. The smallest of these nuclei are initially at near equilibrium with the humidity conditions in their environment. The largest nuclei because of their relatively slow growth are arbitrarily assigned a size which represents a certain lag in adapting to the environment.

The air in the column rises, according to a given function of height and time, increasing or decreasing the relative humidity by adiabatic expansion or compression. The droplets grow, according to the condensation drop growth equation, reducing the relative humidity by consuming water vapor and adding heat to the environmental air.

The relative humidity or supersaturation increases until a level is reached where the consumption of water vapor by the droplets and the latent heat of condensation balance the humidity changes which would result from the adiabatic cooling. At this point of balance the highest supersaturation is reached. This maximum value determines the smallest size of condensation nucleus which will exceed its critical radius according to the classical curves of KÖHLER (1926), which in a revised form are given in figure 1 showing the equilibrium radii for droplets with given nuclei at given relative humidities. Droplets which exceed this critical radius continue to grow as long as the relative humidity exceeds the equilibrium values for the droplets. Droplets which fall short of this critical radius cannot exceed the equilibrium value and will remain on the lower or stable side of the curve.

Therefore when maximum supersaturation is reached, the droplet size spectrum is divided into growing cloud droplets on the one hand and nucleus droplets nearly in equilibrium on the other.

The balance struck between the growing droplets and the humidity changes which result from cooling, is soon altered. As the radii of these droplets increase, their water consumption also increases, until they consume more water than for the balanced condition. The supersaturation is thus reduced gradually following the growth of the particles.

The largest of these droplets will settle noticably against the rising air. If the rate of settling is an appreciable portion of the vertical velocity, the concentration of these particles increases. For any given size of nuclei when the fall velocity of the particles equals the vertical velocity of the air, a high concentration of droplets may exist in a thin horizontal layer which in turn may affect the water consumption for this layer and therefore the humidity conditions. In certain cases, therefore, the maximum humidity or supersaturation is influenced by this increased population of larger drops. This process would be especially important in the lowest few meters of the cloud. Although it is not a part of the phase of the investigation reported here it should be pointed out that coalescence between droplets quite conceivably could by this mechanism exert a strong influence on subsequent droplet growth by condensation. The resulting influence would be to reduce the number of growing droplets as time passes. These fewer droplets therefore will grow faster than the preceding ones.

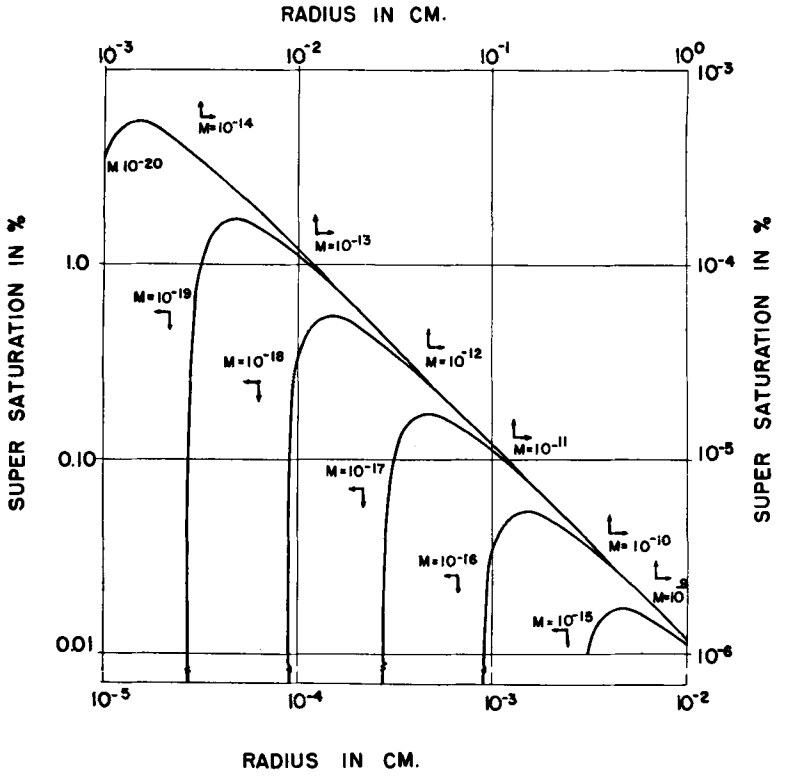

Fig. 1. Köhler type equilibrium curves for droplets formed on given nuclei sizes. Coordinates given at the left and bottom indicate humidity and radius for NaCl nucleus size M in moles indicated at left of curves while coordinates at top and right indicate values for nucleus size indicated at right of curve.

For the sake of simplicity the above remarks have referred to a steady, rising current with a fixed nucleus spectrum. In the model as it is actually used, it is possible to make the vertical velocity a function of time and height and hence better to simulate cloud conditions. The number of condensation nuclei introduced at cloud base can also be altered during the course of the computation. In fact, a variety of circumstances can be studied, i.e. vertical velocity, temperature and humidity, nuclei distribution. The results of some of these altered considerations will be given in a subsequent report.

3. The droplet growth equation

To compute the growth of a droplet in a changing environment of temperature and humidity one must know the rate of diffusion of water vapor to the droplet, and the rate of diffusion of heat away from the droplet Knowing these factors and the heat capacity of the droplet, one can determine its heat-water vapor budget and hence growth.

Evaporation or condensation of the droplet or droplets affects the environment which in turn affects the subsequent particle growth, so no computation of droplet growth is adequate for meteorological purposes which does not consider droplets *in relation to each other and in relation to a changing environment.*

The growth of a droplet by diffusion may be satisfactorily expressed by:

$$\frac{dm}{d_t} = 4\pi r \frac{\varepsilon D}{RT}(e_\infty - e_r) \qquad (1)$$

for a steady state case (for example, JOHNSON 1954):

where m = mass of droplet
ε = ratio of molecular weight of water vapor and air
D = water vapor diffusion coefficient
R = *the gas constant*
T abs temperature
r = droplet radius

The equilibrium vapor pressure over a droplet was derived by KELVIN (1870) and modified and revised for meteorological purposes by KÖHLER (1926). Equations governing the growth of droplets by condensation have been given as well by HOWELL (1949), VIERHOUT (1949), SQUIRES (1953), MASON (1957) and others. The equations, as presented here, differ in certain details following the suggestions of MCDONALD (1953), MASON (1957 a), and ROOTH (1957).

The expression for the equilibrium condition is:

$$e_r = e_{T_r}\left(1 + \frac{2\sigma\varepsilon}{\varrho R T r} - \frac{3iMm_\omega}{4\pi\varrho r^3}\right) =$$

$$= e_{T_r}\left(1 + \frac{A}{r} - \frac{iBM}{r^3}\right) \qquad (2)$$

$$A = \frac{2\sigma\varepsilon}{\varrho R T} \qquad B = \frac{3m_\omega}{4\pi\varrho}$$

where e_r = vapor pressure over the *droplet* surface in bars
e_{T_r} = *saturation* vapor pressure at the temp T_r in bars
σ = surface tension of water at temp T in dynes/cm^2
ε = ratio mol · wt H_2O to dry air = 18/29 = .621
R = gas const = 1.87×10^6 ergs g^{-1} °C^{-1}
T = temp in °K
r = droplet radius in cm
i = van 't Hoff factor (2)
M = wt in moles of condensation nucleus
m_ω = mol wt of water
ϱ = density of water g/cm^3

Two terms in this expression should be specially noted. The first is the term containing A which describes the increase of the vapor pressure over the curved surface of the droplet. The second term is the one containing B which describes the lowering of the vapor pressure by the presence of a solute, in this case assumed to be NaCl, in the droplet.

The ambient vapor pressure, (e_∞), at a distance far enough from the droplet to be unaffected by it we shall presume is the saturation vapor pressure corresponding to the dewpoint temperature of the air. The vapor pressure at the surface of the droplet, (e_r), is the vapor pressure of a droplet of salt solution with a known nucleus size and at the temperature of the *surface* of the droplet. The temperature of the droplet surface cannot be known directly in the condensation process and must be deduced from a consideration of the heat balance of the droplet in a known environment.

a) *Drop temperature*

To do this, one must have a second equation which describes the heat budget of the droplet. The diffusion of heat to or away from a droplet, analogous to equation (1), is given by:

$$\frac{dQ}{dt} = 4\pi r k(T_\infty - T_r) \qquad (3)$$

where k = thermal diffusion coefficient
$\frac{dQ}{dt}$ = the heat flux inwards through the droplet surface
T_∞ = the temperature of the environment at a sufficient distance to be unaffected by the droplet
T_r = the temperature of the droplet surface

To determine the droplet temperature we may consider that the heat gained by condensation, less the heat lost by heat diffusion, equals the change in heat stored in the droplet, i.e.

$$L\frac{dm}{dt} + \frac{dQ}{dt} = \frac{4}{3}\pi r^3 \varrho c \frac{dT_r}{dt} \qquad (4)$$

c = specific heat
ϱ = density of liquid water
L = latent heat of evaporation of water

Strictly, T_r, should be the average temperature within the droplet but it has been written

here as approximated by the surface temperature. The term containing $\frac{dm}{dt}$, as taken from equation (1), is expressed in terms of the vapor pressure. The objective here is to express the drop temperature in terms of the ambient temperature and dew point. This is done by use of the Clausius-Clapeyron equation, that is

$$\frac{1}{e}\frac{\Delta e}{\Delta T} = \frac{\varepsilon JL}{RT^2}$$

or

$$e - e_0 \approx \frac{\varepsilon JLe}{R\bar{T}^2}(T - T_0) \qquad (5)$$

if $\Delta e \ll e$

where J = mech. equiv. of heat,
e, e_0 = vapor pressure at T, T_0

Using equation (5) as:

$$e_{T'} - e_{T_r} = \frac{\varepsilon JLe}{R\bar{T}^2}(T' - T_r)$$

where T' = dew point temperature
$e_{T'}$ = sat. vapor pressure at T'
e_{T_r} = sat. vapor pressure at T_r

and the equilibrium vapor pressure over a droplet of dilute salt solution written as:

$$e_r = e_{T_r}\left(1 + \frac{A}{r} - \frac{iBM}{r^3}\right)$$

we can write that:

$$e_{T'} - e_r = \frac{e\varepsilon JL}{RT^2}\left(T' - T_r - \frac{A^\star}{r} + \frac{iB^\star M}{r^3}\right) \qquad (6)$$

where

$$A^\star = \frac{RT^2}{\varepsilon JL}A$$

$$B^\star = \frac{RT^2}{\varepsilon JL}B$$

and $\frac{e_{T_r}}{e}$ is taken ≈ 1 when multiplied by $\left(\frac{A}{r} - \frac{iBM}{r^3}\right)$

If we substitute this in equations (1) and (4) we have then:

$$\frac{4}{3}\pi r^3 c\frac{dT_r}{dt} + 4\pi rk(T_r - T_\infty) =$$

$$= L\cdot\frac{\varepsilon D}{RT}\left[\frac{\varepsilon JLe}{RT^2}\left(T' - T_r - \frac{A^\star}{r} + \frac{iB^\star M}{r^3}\right)\right] \qquad (7)$$

where $\varrho_\omega = 1$.

This gives us an equation from which we can determine the drop temperature from the ambient temperature and the dew point temperature. From (7) we write:

$$c_1\frac{dT_r}{dt} + c_2(T_r - T_\infty) = + c_3(T'^\star - T_r)$$

where

$$c_1 = r^2/ec$$

$$c_2 = k$$

$$c^3 = \frac{L\varepsilon D}{RT}\left[\frac{\varepsilon DLe}{RT^2}\right]$$

$$T'^\star = T' - \frac{A^\star}{r} + \frac{iB^\star M}{r^3}$$

Howell (1949), Squires (1952) and Arons and Keith (1954) have pointed out, however, that a complete solution to this equation is unnecessary as the heat capacity of the droplet may be neglected. Writing this equation as

$$T_r = \frac{c_3 T'^\star + c_2 T_\infty}{c_3 + c_2} + \frac{1}{c_3 + c_2}\frac{dT_r}{dt} \qquad (8)$$

the second term on the right side of equation (8) indicates the lag in temperature of the droplet due to its heat storage. The rate $\frac{dTr}{dt}$ can not be expected to be much larger than the rate of change of the temperature of the environment $\frac{dT_\infty}{dt}$ which can easily be estimated. For drops less than 100 μ therefore the lag will not exceed $\pm$ .005° C assuming a lapse rate of 0.01° C/m and a vertical velocity of 3 m/sec and will be 5×10^{-6}° C for 10 μ

droplets. This is negligible in relation to the other terms.

From equations (1), (2), (5) and (8) we can now write

$$\frac{dm}{dt} = 4\pi r \frac{\varepsilon D}{RT}(e_\infty - e_r) =$$

$$= 4\pi r \frac{\varepsilon D}{RT}(e_\infty - e_s + e_s - e_r)$$

Here we shall designate e_s to mean the saturation vapor pressure at the ambient temperature T_∞ (i.e. corresponds to the saturation mixing ratio as opposed to the actual mixing ratio).

From equation (5) we can write,

$$e_s - e_r = e_s - e_{T_r}\left(1 + \frac{A}{r} - \frac{iBM}{r^3}\right)$$

From equation (5)

$$e_s - e_{T_r} = \frac{\varepsilon JLe}{RT^2}(T_\infty - T_r)$$

From equation (8), by omitting the term containing $\frac{dT_r}{dt}$,

$$L\frac{dm}{dt} = 4\pi kr(T_\infty - T_r)$$

Combining these expressions we get

$$e_s - e_{T_r} = \frac{\varepsilon JLe}{RT^2} \cdot \frac{L}{4\pi kr}\frac{dm}{dt}$$

The growth equation then becomes

$$\frac{dm}{dt} = 4\pi r \frac{\varepsilon d}{RT}\left[e_\infty - e_s - e_{T_r}\left(\frac{A}{r} - \frac{iBM}{r^3}\right)\right] +$$

$$+ \frac{4\pi r \varepsilon D}{RT} \cdot \frac{\varepsilon JL^2 e}{kRT^2} \cdot \frac{1}{4\pi^2}\frac{dm}{dt}$$

or

$$\frac{dm}{dt} = \left(\frac{1}{1 + \frac{\varepsilon^2 JL^2 De}{kR^2T^3}}\right) 4\pi r \frac{\varepsilon D}{RT}$$

$$\left[e_\infty - e_s - e_{T_r}\left(\frac{A}{r} - \frac{iBM}{r^3}\right)\right]$$

In the last term of the expression e_{T_r} can be replaced by e_s without seriously changing the results since it is the difference between $\frac{A}{r}$ and $\frac{iBM}{r^3}$ which is the dominating quantity here. In this way the equation takes the form

$$\frac{dm}{dt} = 4\pi r \frac{\varepsilon D}{RT}\left(\frac{1}{1 + \frac{\varepsilon^2 JL^2 De}{kR^2T^3}}\right) \cdot$$

$$\cdot \left[e_\infty - e_s\left(1 + \frac{A}{r} - \frac{iBM}{r^3}\right)\right] \qquad (9)$$

The term

$$\left(\frac{1}{1 + \frac{\varepsilon^2 JL^2 De}{kR^2T^3}}\right)$$

indicates the modification of the vapor pressure difference between the droplet and the environment caused by the heating associated with the droplet growth.

b) *The vapor pressure reduction due to the dissolved nucleus*

The nuclei used in the present computations are assumed to be composed of sodium chloride while the numbers of these nuclei correspond to the numbers of *sea salt* particles as measured by WOODCOCK (1949), MOORE and MASON (1957), or in the case of the very smallest particles by JUNGE (1952). It is necessary therefore to compare the reduction in vapor pressure over solutions of sea salt and sodium chloride to see how well they correspond at concentrations implied by the droplet sizes involved in the computations.

The vapor pressure reduction over sea salt solutions has been investigated in some detail by ARONS and KIENTZLER (1954). It will therefore suffice to compare the reduction in vapor pressure of NaCl as indicated in the growth equation (9), with the values they determined empirically, to establish the accuracy of the assumption made in the computation.

As computed in the growth equation, the reduction in vapor pressure due to the presence of the salt nucleus is an approximate form of

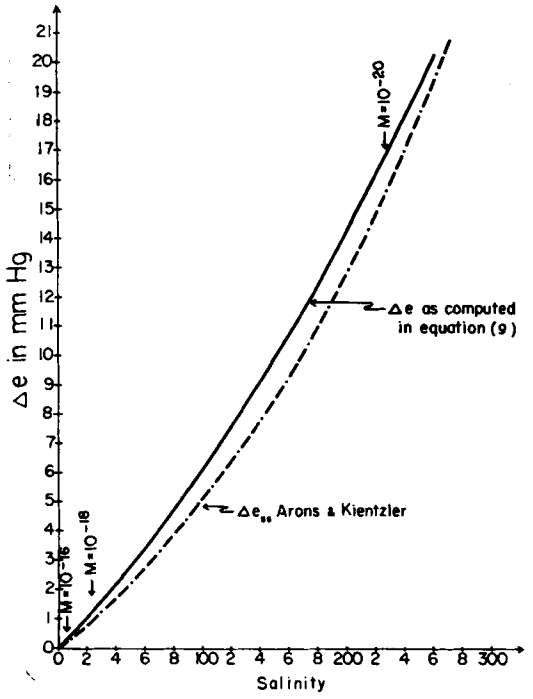

Fig. 2. The reduction of vapor pressure over sea salt solution of varying salinity (Arons and Kientzler) and over solutions of NaCl as assumed in the computations here. Concentrations found in small droplets in equilibrium with 100 % rel. hum. are indicated by arrows along the curve.

Raoult's Law as modified by the van 't Hoff factor, i.e.

$$\frac{\Delta e}{e} = \frac{im_s}{im_s + m} \approx \frac{im_s}{m}$$

or

$$\frac{\Delta e}{e} = \frac{iMm_\omega}{\frac{4}{3}\pi r^3 \varrho}$$

as given in equation (9).

Therefore, if we plot Δe as computed in this approximate form to $\Delta e_{(\text{sea salt})}$ as measured by Arons and Kientzler, we can estimate the error caused by assuming a NaCl nucleus. This has been done in figure 2 for 10° C. Salinity in the case of the empirical data is computed in the usual way from the chlorinity (sal $= 0.03 + 1.805$ cl, SVERDRUP ET AL, 1942). Salinity as *computed* was the approximate value m_s/m rather than $\frac{m_s}{m_s + m}$. The van't Hoff factor varies from 1.82 to 2.91 according to MCDONALD (1953) in the range of values considered, but in these computations it was considered constant, $i = 2$.

The computed values of Δe are not more than 15 % from the empirical sea salt values, which is not a serious factor in the computations in view of the uncertainties concerning the exact chemical composition of the nuclei. Analyses of rainwater such as reported by ERIKSSON (1952) and MORDY (1953) indicate that salts do not appear in rainwater in the same ratio as in sea water. Furthermore, while the assumption that the nuclei are sea salt may be relatively safe in the case of the very large nuclei as measured by WOODCOCK, the smaller particles as has been shown by JUNGE (1952) and others, may consist of a variety of substances. These smaller particles sometimes consist of highly concentrated solutions even at 100 % relative humidity due to the size of the capillarity term A/r in the growth equation (10) below.

It will later be shown that the dominant factor in the initial condensation process in determining the environmental humidity and therefore droplet number for a given nucleus distribution, is the rate of cooling, and that in consideration of this controlling factor, small errors in the nucleus term are relatively unimportant.

c) *Ventilation*

The work of FRÖSSLING (1938) shows that the modification of this equation necessary to provide for ventilation of the droplets is given by empirically determined coefficients to the diffusion equations, i.e.

$$\frac{dm}{dt} = 4\pi r \frac{\varepsilon D}{RT}(e_\infty - e_r)F_1$$

$$\frac{dQ}{dt} = 4\pi r k(T_\infty - T_r)F_2$$

where

$$F_1 = F_1(R_e, \sigma) = 1 + 0.276 \sqrt[3]{\sigma}\ \sqrt{R_e}$$

$$F_2 = F_2(R_e, \sigma') = 1 + 0.276 \sqrt[3]{\sigma'}\ \sqrt{R_e}$$

and R_e = Reynold's number.
σ = Prandtl's number.
$\sigma' = \nu/D$

when these ventilation coefficients are introduced in the equations above, equation (9) becomes:

$$\frac{dm}{dt} = 4\pi r \frac{\varepsilon D}{RT} F_1 \left[\frac{1}{1 + \frac{\varepsilon^2 JL^2 De}{kR^2T^3}}\right] \cdot \left[e_\infty - e_s\left(1 - \frac{A}{r} + \frac{iBM}{r^3}\right)\right] \quad (10)$$

Errors due to the omission of the ventilation terms are not serious before the radius exceeds 30 microns. In the experimental measurements of droplet growth of KEITH and ARONS (1954), they conclude that it is not important for droplets of a radius less than 50 or 60 microns.

d) *Diffusion coefficients for small droplets*

ROOTH (1957) has shown that for small droplets, $r < 5\ \mu$, the condensation coefficient of water molecules on a water surface becomes an important factor in determining the rate of droplet growth.

In the case of equilibrium

$$q_e = \beta q_c$$

where q_e = molecules escaping surface
q_c = molecules colliding with surface
β = condensation coefficient

From gas kinetics

$$q_c = \frac{e}{\left(\frac{2\pi RT}{\varepsilon}\right)^{\frac{1}{2}}} \text{ and the refore } q_e = \frac{\beta e_0}{\left(\frac{2\pi RT}{\varepsilon}\right)^{\frac{1}{2}}}$$

If the evaporation

$$q = q_e - \beta q_c$$

$$e = e_0\left(1 - \frac{q}{\beta q_e}\right)$$

For a sphere, as in equation (1)

$$\frac{dm}{dt} = -4\pi r^2 q = 4\pi r^2 \frac{\varepsilon D}{RT}\left(\frac{e_\infty - e_r}{r}\right)$$

But

$$e_r - e_s = \frac{-qe_0}{\beta q_e} = \frac{-q}{\beta}\sqrt{\frac{2\pi RT}{\varepsilon}}$$

$$= \frac{e_\infty - e_r}{r} \cdot \frac{\varepsilon D}{RT\beta}\sqrt{\frac{2\pi RT}{\varepsilon}}$$

If we let

$$l = \frac{D}{\beta}\sqrt{\frac{2\pi\varepsilon}{RT}}$$

then

$$e_r - e_s = \frac{l}{r}(e_\infty = e_r)$$

Eliminating we get

$$\frac{dm}{dt} = 4\pi r^2 \frac{\varepsilon D}{RT}\left(\frac{e_\infty - e_0}{l + r}\right)$$

If the droplet radius is comparable to or smaller than the mean free path in the surrounding gas, then a further correction for the geometry of the collisions has to be made.

Although the values for β are difficult to determine and are therefore somewhat uncertain, using the values at hand, Rooth calculates, with $\beta = .036$ at 10° C (Alty and Mackay), that $l = 5.1\ \mu$

If we therefore apply this correction $\left(\frac{r}{r+l}\right)$ to the diffusion coefficient, we find that its values differ markedly from Langmuir's values as used by Howell and Squires.

LANGMUIR's (1944) corrections to the diffusion coefficients are given as:

$$\frac{1}{D'} = \frac{r}{D(r + a\lambda)} + \frac{1}{r}\sqrt{\frac{2\pi\varepsilon}{RT}}$$

D' = modified diffusion coefficient
a = Cunningham constant
λ = mean free path of water molecules in air.

In the above expression the first term is for the purpose of correcting for the geometry of capture of the molecules. The second term is the same as described by Rooth except that a has been assumed to be $a = 1$. If this expression is put in comparable form to the expressions above, we find

$$\frac{1}{D'} = \frac{1}{D}\left[\frac{r}{r + a\lambda} + \frac{\varepsilon D}{rRT}\sqrt{2\pi RT}\right]$$

$$= \frac{1}{D}\left[\frac{1}{1 + \frac{a\lambda}{r}} + \frac{\beta}{r}\right]$$

or, $$D' = D\left[\frac{r\left(1 + \frac{a\lambda}{r}\right)}{r + \beta l\left(1 + \frac{a\lambda}{r}\right)}\right]$$

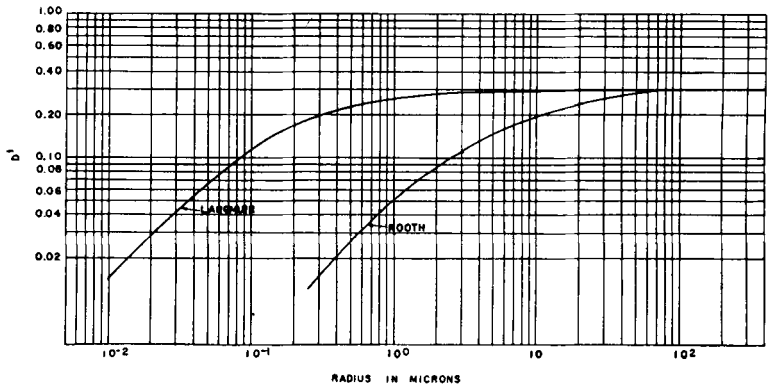

Fig. 3. A comparison of the correction to the water vapor diffusion coefficient for small droplets as used by Langmuir and Howell, and the values used here as derived by Rooth.

while Rooth's expression is:

$$D' = D\left[\frac{r}{r+l}\right]$$

It should be noted here that the term

$$\left(1 + \frac{a\lambda}{r}\right)$$

is important only when $a\lambda$ is comparable to r. As

$$\lambda \approx 10^{-5} \text{ cm} \quad \text{and} \quad a = 0.7$$

this term becomes important for droplets $< 0.1\ \mu$ but has been neglected in the present computations.

By analogy the heat diffusion coefficient is written:

$$\frac{1}{k'} = \frac{1}{k}\left[\frac{1}{1 + \frac{a\lambda}{r}} + \frac{4k}{r\varrho_a c_p f}\sqrt{\frac{\varrho_v}{3\bar{e}}}\right]$$

Graphs of the values of the water vapor diffusion coefficients for different values of r are given in figure 3.

e) *Final equation*

After these considerations, the droplet growth equation as used in the computation is written

$$\frac{dm}{dt} = 4\pi r^2 \varrho \frac{dr}{dt} = 4\pi\left(\frac{r^2}{r+l}\right)\frac{\varepsilon D}{RT}F_1 \cdot$$

$$\left(\frac{1}{1 + \frac{\varepsilon^2 JL^2 De}{kR^2T^3}}\right)\left[e_\infty - e_s\left(1 - \frac{}{r} + \frac{iBM}{r^3}\right)\right] \quad (11)$$

The term $\frac{F_1}{F_2}$ as it occurs in the temperature feedback term $\left[\frac{1}{1 + \frac{\varepsilon^2 JL^2 De}{kR^2T^3}\left(\frac{F_1}{F_2}\right)}\right]$ is very nearly equal to one in the particle size range involved in the computations and has been neglected.

4. Computational procedure

Numerical computations were accomplished by the following stepwise procedure.

1) cooling the parcel containing the droplet (i.e. reducing p),
2) computing droplet growth,
3) computing humidity and temperature changes,
4) computing droplet settling and position,
5) introducing new droplets at the cloud base,
6) repeating the process.

This is indicated in the block diagram given in fig. 4.

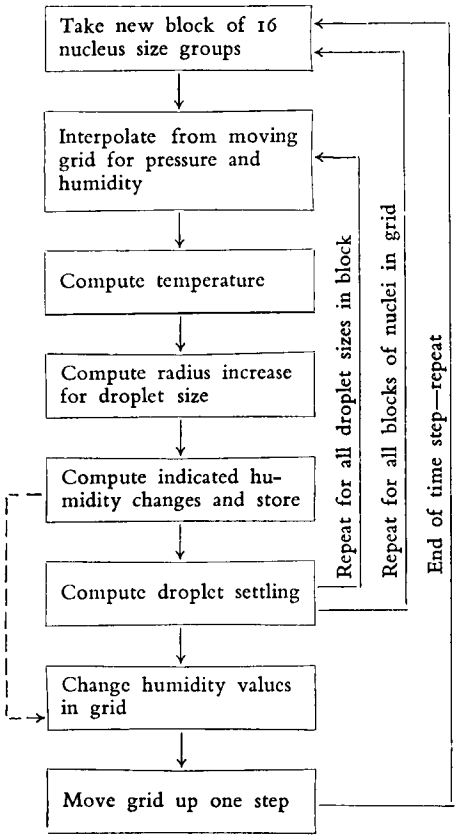

Fig. 4. Block diagram for computing sequence.

The position of the droplets was defined with respect to a grid moving upward with the same speed as the vertical wind velocity. Each fourth time step a new grid level was added at the bottom of the column. Each time step a new block of nuclei was added to the base of the column. The nucleus distribution was represented by this block of 16 sizes (values of M) or groups of nuclei with the number of particles assigned to each of these groups according to the different nucleus distributions assumed. Values of the environmental temperature and humidity, which were obtained for the growth of the nuclei, were determined by appropriate interpolation in this moving grid system. Humidity and temperature corrections due to condensation were apportioned to the immediate upper and lower grid level above and below the droplets according to the position of the droplets between the levels. These corrections were summed for all droplets through one time step before they were applied at each level.

a) *Temperature changes*

The temperatures of the individual air parcels were determined by interpolation from the moving grid system. Temperature changes on this grid were accomplished by computing the adiabatic change in temperature (approximated) for the increment in pressure assumed for each time step, and correcting this change by the latent heat released as indicated by the change in mixing ratio resulting from the condensation on the droplets. These changes in the mixing ratio were made by dividing the condensed water on each size group of droplets between the upper and lower grid level according to the droplets' position between the grid levels. The change in the mixing ratio at the end of each time step was the sum of all such corrections for droplets in the levels lying just above or below the grid level in question.

The adiabatic temperature change was approximated by a linear expression so that temperature changes were computed by

$$T_\infty = T_0 + K_1(p - p_0) + K_2(x - x_0)$$

where T_∞ = the temperature
p = pressure
x = mixing ratio.
The constant K_1 = the average dry adiabatic lapse rate assumed for the pressures used ($\approx 0.1^\circ$ C/mb).
K_2 = the latent heat of evaporation divided by the density and specific heat of the air.

Buoyancy effects due to heat changes were not considered as the air was displaced vertically according to assumed rates of rise.

b) *Droplet growth*

As indicated in sections 4 and 6, droplets were classified according to the size of their nucleus. Droplet radius and pressure level (i.e. location) were stored in the computer, the appropriate nucleus size and number being indicated by the storage cell where this information was kept. As needed for droplet growth computation, pressure, temperature

and humidity were obtainable from the grid system; radius, nucleus size, and droplet height location from the stored blocks of nuclei information.

The droplet growth equation (11) in finite difference form was written simply,

$$\Delta r = \Delta t \cdot F_1 \cdot \alpha \left(\frac{1}{1 + \frac{l}{r}} \right) \cdot$$

$$\cdot \left[px - \varepsilon e_s \left(1 + \frac{A}{r} - \frac{2BM}{r_3} \right) \right] \qquad (12)$$

where

$$\alpha = \frac{D}{RT} \left[\frac{1}{1 + \frac{\varepsilon^2 JL^2 De}{kR^2 T^3}} \right] \approx \alpha_0 +$$

$$+ \frac{\partial \alpha}{\partial T} dT = \alpha_0 + \alpha_1 \Delta T$$

where $\Delta T = T_\infty - T_0$

and e_∞ was approximated from $x = \frac{\varepsilon e_\infty}{p - e_\infty} \approx \frac{\varepsilon e_\infty}{p}$

The saturation vapor pressure e_s was determined from an empirical expression derived from the saturation vapor pressure data, that is,

$$e_s = e_0 + \frac{\partial e}{\partial T} dT + \frac{\partial^2 e}{\partial T^2} dT^2 =$$

$$= e_0 + e_1 \Delta T + e_2 \Delta T^2$$

the values of e_1, and e_2 being computed from the vapor pressure tables appropriate to the initial conditions.

c) *Droplet sedimentation*

Droplet motion was assumed to be determined by Stoke's law, that is,

$$v = \omega - \frac{2\varrho g r^2}{q\eta} \approx \omega - kr^2$$

where ω = the vertical velocity of the air current
ϱ = density of water
g = gravitational acceleration
η = coefficient of viscosity of air

This assumption is reasonable as long as the droplets are less than 40 μ in radius (GUNN and KINZER 1949).

5. Special problems in the computation

The rate at which very small droplets react to changes in the ambient humidity is extremely fast and this fact necessitates quite short time steps and small changes in the humidity during the computations. However, once the term containing the nucleus diminishes in importance, i.e. when the droplets reach their critical radius $\left(r_c = \sqrt{\frac{3iBM}{A}} \right)$ on the Köhler equilibrium curves fig. 1, growth proceeds more slowly. A limitation in the length of time step which can be taken occurs when the changes indicated in pressure, humidity, and temperature for a given time step are too small for accurate representation in the storage of the computer. Furthermore, due to the storage capacity of the BESK computer, the length of the computations is limited to 256 time steps or 64 grid levels. If very short time steps are chosen, computations can only proceed for only a very short drop growth period. A useful measure of this time scale is given by the time constant, the time it would take a droplet not in equilibrium with an environment of constant temperature and humidity, to decrease its deviation from equilibrium by a factor 1/2.718.

The time constant as computed is:*

$$t_0 = \frac{1}{-\frac{1}{\Delta r}\frac{d(\Delta r)}{dt}} - \approx \frac{1}{\frac{\partial}{\partial r}\left(\frac{dr}{dt}\right)} \text{ where } \Delta r = r - r_c$$

$$\frac{\partial}{\partial r}\left(\frac{dr}{dt}\right) \approx \frac{\partial}{\partial r}\left(\frac{\alpha}{r}\right)\left[e_\infty - e_s \left(1 + \frac{A}{r} - \frac{iBM}{r^3} \right) \right]$$

$$\approx -\frac{\alpha}{r^2}\left[e_\infty - e_s \left(1 + \frac{2A}{r} - \frac{4iBM}{r^3} \right) \right]$$

$\alpha \approx$ const

At 100 % R.H., $e_\infty = e_s$ and for a nucleus droplet in equilibrium $\frac{A}{r} = \frac{iBM}{r^3}$

* In these expressions the corrections of the water vapor diffusion coefficient have been omitted, they become important when the nucleus size $M < 10^{-17}$. However for sizes smaller than this the time constant is very small and variation in the time constant due to these corrections have little significance in the present computations.

Therefore

$$t_0 = \frac{r^5}{2\alpha iBMe_s} = \frac{(iBM)^{3/2}}{2\alpha A^{3/2} e_s} \approx 1.9 \times 10^{24} (M)^{3/2}$$

Characteristic values of t_0 are given in table 1.

Table 1. Time constants for various nucleus sizes at 100 % humidity.

M	10^{-12}	10^{-13}	10^{-14}	10^{-15}	10^{-16}	10^{-17} moles
t_0	1.9×10^6	58×10^6	1.9×10^8	58	1.9	.058 seconds

At the critical radius on the equilibrium curves, fig. 1, $t_0 = \infty$, i.e.

$$\frac{de}{dr} = 0, \quad \frac{A}{r_c^2} = \frac{3iBM}{r_c^4}, \quad e_\infty - e_s = \frac{2iBMe_s}{r^3}$$

It is easily shown that the time constants lengthen as the particles grow.

The nuclei used in the computations ranged in size from $M = 10^{-10.2}$ to $M = 10^{-19.2}$. For the smallest nuclei therefore it was not possible to use time steps short enough to overcome the problem of their very rapid growth.

It was possible to circumvent this problem by comparing the computed droplet growth for each change in humidity with an approximate growth amount taken from its equilibrium value before and after the change in humidity. If the computed growth was too large (i.e. $8\Delta r > r$) then the equilibrium value appropriate to the environmental humidity was substituted. It was found that this was necessary only for $M < 10^{-17}$ in the first part of these droplets' growth. By the time the droplets reached their critical radii, their growth was being computed by the growth equation. This method seems quite practical since with such short time constants the radii of these small droplets can never differ appreciably from their equilibrium radii in early stages of growth at *observed rates of rise in clouds*, and little error in the computations can result.

6. Conditions chosen for study

As indicated above, the distributions examined by HOWELL (1949) were for nuclei smaller than those since found also important, WOODCOCK (1953, 1955), MOORE and MASON (1957). Woodcock has related the distribution of these larger ($M = 10^{-11}$) particles at cloud base level to wind velocity and measured their vertical distribution over the sea. As mentioned above the nucleus distributions for the larger particles as used in the computations were largely taken from his data. The smaller nucleus data were representative values taken from the work of Junge.

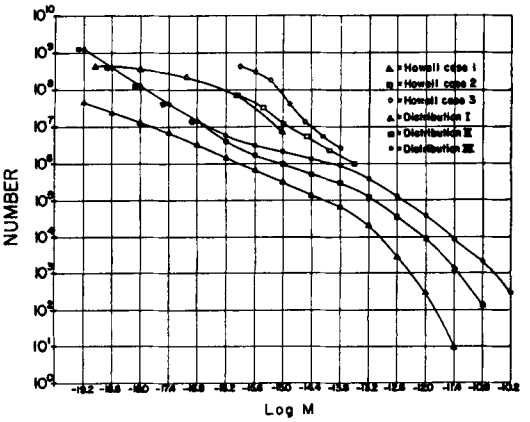

Fig. 5. The cumulative numbers of the nuclei used in the computations indicated opposite the logarithm of their weight in moles—open symbols indicate the distributions used earlier by Howell.

The distributions used in the computations together with those used by Howell are shown for comparison in figure 5. For the purpose of comparing the computations here with Howell's earlier work, computations were also made with his Case 1 and Case 3 distributions. His Case 2 could not be checked due to the assumption of a 1.5 cm/sec vertical velocity which required computing accuracy not available in the computer program as written.

The distributions given in figure 4 are designated Distribution I, II, III, corresponding to low, moderate or high concentrations of large salt particles ($M = 10^{-13.8}$) as measured by Woodcock in Hawaii and elsewhere. They approximately correspond to the salt distributions which he gives as characteristic for days where the wind force was Beaufort force 1, 4, and 7 respectively.

The objective of this study was to determine the range of cloud particle sizes implied by the observed ranges in nucleus sizes and cloud vertical velocity. Comparison of these results with recent cloud droplet size data

then should allow some separation of the condensation process from other processes such as turbulence, coalescence, and freezing. To do this, the range of particle numbers indicated in Woodcock's measurements characteristics of distributions for Beaufort wind force 1, force 4, and force 7, were extended arbitrarily into the Junge-Aitken range of smaller particles. These extended distributions were then assigned initial radii.

a) *The radii of nuclei at cloud base*

The largest nuclei measured by Woodcock were more than $M = 10^{-10}$ moles. Such particles require days (see table 1) to come to their equilibrium radii at 100 %. In fact their equilibrium radii are so large that it is unlikely that they would remain supported in the air at this level for a large fraction of the length of time required to reach equilibrium. The smallest nuclei ($M = 10^{-16}$), however, reach their equilibrium radii in seconds or fractions of a second. It is safe therefore to assume that for smaller sizes, the initial radii used in the computations should be their equilibrium size at the assumed *initial* relative humidity some distance below cloud base.

To determine precisely the radii of the large particles at cloud base, however, one should know the history of the individual particle, for with varied humidity in the sub-cloud layer and the probable turbulent transfer of these particles from sea surface to cloud level, each particle would arrive after a different travel time. This travel time of course is not possible to measure practically, and certain assumptions must be made concerning the level from which the particles are drawn into the cloud, the humidity and the velocity with which they are brought up. The assumption of uniform size for particles with a given larger M value is therefore probably in serious error. Initially these largest nuclei, due to their small numbers do not noticably affect the growth of the smaller particles however.

Woodcock has also measured the number of particles at various levels above the sea surface. From his data it is possible to estimate, using turbulent transfer theory, characteristic sizes of the nucleus droplets at each level. For example, from these data one obtains an estimate of $\frac{dN(M)}{dz}$, the change in number of a particular nucleus size M with increasing height Z. For a steady state

$$\frac{\partial N_m}{\partial t} = \frac{\partial}{\partial z}\left(K\frac{\partial N_m}{\partial z} + v_m N_m\right) = 0$$

where v_m = velocity of fall of the M size particles = cr_m^2 and K = the exchange coefficient. From this we write,

$$K\frac{\partial(\log N)}{\partial z} = cr^2$$

In reality of course K varies considerably with height, wind velocity, and stability. The assumption that the vertical flux is zero is also made here, so this is admittedly a crude estimate.

If we take $\bar{K} = 10^{-5}$ cm^2/sec^{-1}, a value commonly used over the sea at levels well above the boundary layer, and take $\frac{\partial(\log N)}{\partial z}$ from Woodcock's measurements during project shower (Tellus 1957), we obtain values for $r_m(z)$. The values obtained in this way represent the radius corresponding to the average rate of fall (cr^2) or therefore represent the root mean square radius.

The values of r_m calculated, and r_{me} in equilibrium with the relative humidity at 99 % and 100 % are given in figure 6 for comparison with the actual initial conditions chosen for study. Interestingly, the radii of the droplet formed on the largest salt nuclei collected near cloud base, as estimated in this way, were smaller than expected due to unexpectedly high numbers of particles at this level. Consequently this estimate at the large end of the spectrum cannot be used. The higher numbers of particles suggest that two or more mechanisms rather than just one may be important in the production of the larger particles. This is to say that in addition to the surf and foam at the sea surface, the coalescence and evaporation of cloud droplets is probably important also in producing significant numbers of the largest nuclei.

However, the values of the initial radii of the rest of the droplets appear to be reasonable both in terms of:

1) the humidity gradient in the sub cloud layer and

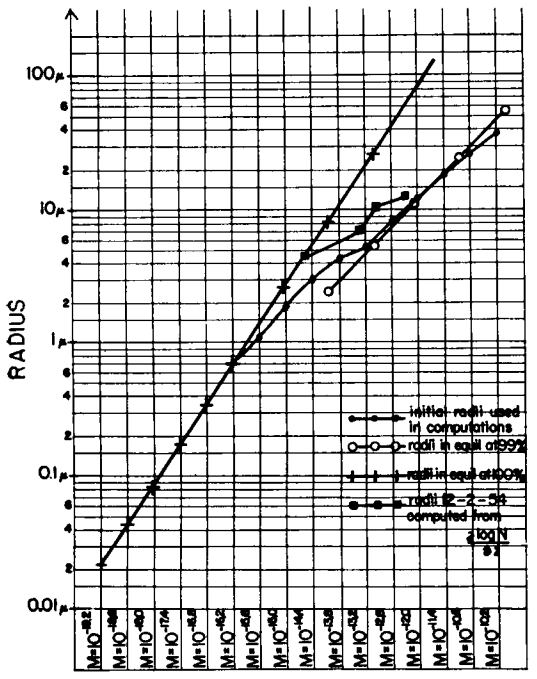

Fig. 6. Initial radii for nuclei droplets used in the computation. Line with (+) symbols indicates radii of droplets if in equilibrium with 100 % R.H. Open circles indicate radii of large particles if in equilibrium with 99 % R.H. Black dots indicate actual radii sizes used for larger particles. Radii for smaller particles were taken from 100 % values. Square symbols indicate radii calculated from turbulence theory and based on observed decrease in number upwards from sea surface.

2) the turbulent transfer of these particles upward.

If, however, an appreciable number of *larger* salt particles is produced by the coalescence and subsequent evaporation of cloud droplets, then these particles should be somewhat larger than those formed on the same size nucleus *ascending* from the sea surface due to the long time constants. Such a case has not been considered here.

Radii of the droplets formed on particles $M = 10^{-15.6}$ and smaller were assumed to be at equilibrium at 100 % relative humidity. Those droplets formed on particles $M = 10^{-12.6}$ and larger were assigned radii appropriate to equilibrium at 99 % relative humidity and those between at intermediate values as shown in the figure.

b) *Vertical velocity, temperature and pressure*

A summary of the conditions for which computations have been made to date are given in table 2.

Table 2

Nucleus distribution	Vertical velocity cm/sec	T_0 °C	P_0 mb	Rel. Hum. %
1. Howell Case 1	60	0	800	100
2. Howell Case 3	30.2	0	800	100
3. Distribution I	15	10	800	100
4. Distribution I	100	10	800	100
5. Distribution II	15	10	800	100
6. Distribution II	50	10	800	100
7. Distribution II	100	10	800	100
8. Distribution III	5	10	800	100
9. Distribution III	15	10	800	100
10. Distribution III	100	10	800	100

The two Howell cases were computed with the present model to compare the differences in machine computing methods with Howell's hand computations, and as a control for accuracy. For case No. 1 the comparison was excellent (Fig. 7) considering that the exact values of the constants as well as the initial radii of the droplets selected by Howell were not precisely known. In case No. 3 (fig. 8) results were also qualitatively the same, but some discrepancies appear probably due to the fact that the initial radii used in the two computations were somewhat different.

In computing the other cases, the initial temperature (10°) and pressure (800 mb) and the initial radii selected were all the same for the purpose of comparing the cases with each other. Vertical velocities chosen ranged from 5 cm/sec to 100 cm/sec. The effects of *varying* vertical velocity *during the ascent* and of varying the nucleus distributions during the course of the computations have been left for a later study. The range of vertical velocities was chosen to demonstrate the most likely differences in the drop size spectrum which result from condensation. Due to the longer time constants for the larger particles, slower rates of rise do not allow the initial differences in radii to be overcome so readily as the more rapid rates of rise. Consequently very slow rates of rise produce the greatest differences in drop radius formed on a given pair of large nucleus sizes. Such differences represent differences in fall velocity and conse-

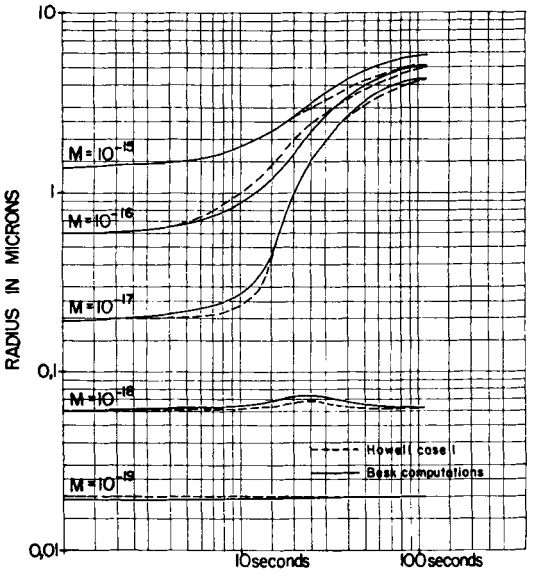

Fig. 7. A comparison of Howell's case 1 computation with computations made here with same initial conditions and nuclei distribution (ω = 60 cm/sec, T_0 = 0° C, P_0 = 800 mb).

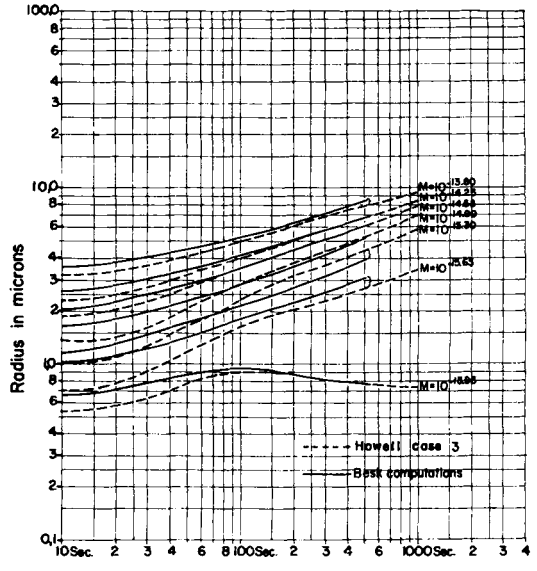

Fig. 8. Comparison of Howell's case 3 with present computations. (ω = 30.2 cm/sec, T_0 = 0° C, P_0 = 800 mb).

quently coalescence probability and thus are primary concern of this study.

Rates of rise in excess of 1 m/sec yield a more nearly uniform drop size spectrum than lower rates as will be shown in section 7 b and the interest in such computations from the standpoint of subsequent coalescense diminishes accordingly.

In the process of testing the machine program for the BESK computer a number of errors occurred which showed that large variation in the main coefficient of the drop growth equation (α in equation 12 for example) produced relatively small changes (comparable to doubling the vertical velocity) in the results of the computations. This is tantamount to saying that even if the rate of growth of the individual particles as indicated by the equation is, for example, doubled, the number and radii of the growing droplets is not dramatically changed due to the feedback on the ambient humidity. For this reason, the initial pressures and temperatures were not changed during the course of the present study.

It might have been interesting to have varied the relative humidity (that is to start computations below cloud base) and/or the initial radii sizes, but choosing suitable and realistic conditions for such computations is more difficult, since the exact nature of the nuclei present is not well known. However, certain experimental calculations of this nature are planned in connection with further work.

7. Some remarks on the results of the computations

With the foregoing considerations in mind we shall now look at two main aspects of the study, that is

1) the differences produced by the various nucleus distributions and

2) the effects of different vertical velocities.

The cases which have been computed, as given in table 2, may be thought of in this reference as constituting a contingency table representing several vertical velocities on one coordinate, and the three nucleus distributions on the other.

In discussing the computations it is helpful if certain classical considerations in the process are borne closely in mind. In the initial condensation on the entire nucleus spectrum, condensation occurs preferentially (i.e. dm/dt is larger) on the larger droplets due to the fact that the radius enters the equation as a multiplying factor. This tendency is further accent-

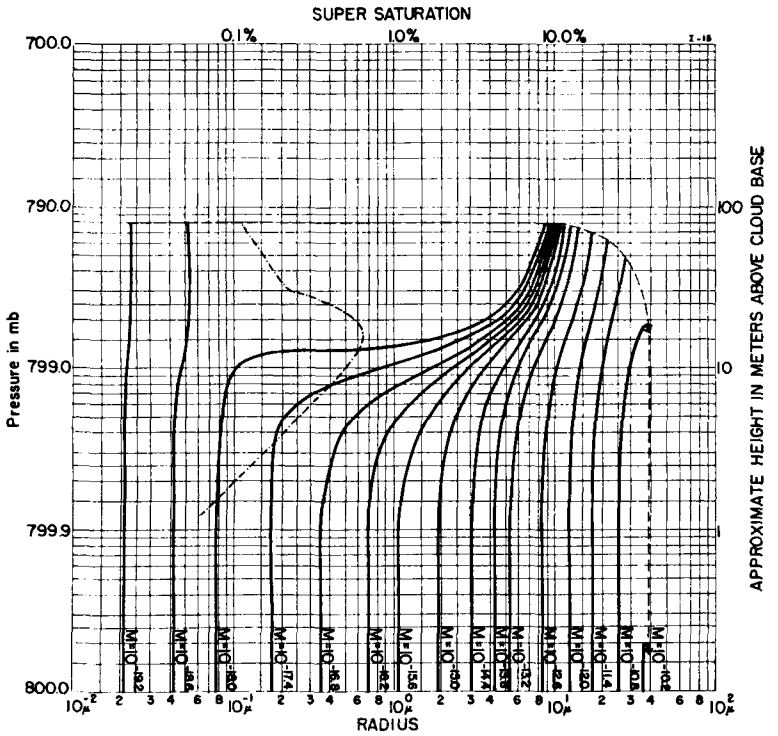

Fig. 9. Results of computation for sparse nucleus concentration, Distribution I at 15 cm/sec rate of rise. Initial radii and nucleus size are given at bottom of graph. Dashed line indicates supersaturation in % at appropriate heights, as given at top of graph.

uated if, as is the general case, these larger droplets, due to their long time lag, are well below their equilibrium radii for the ambient humidity. For a steady rate of cooling, if the number of these particles is sufficiently large, they will consume water rapidly enough to prevent the humidity from increasing. If not, the humidity will rise. As is well known, for given temperatures a maximum attainable equilibrium vapor pressure value exists for each nucleus size, corresponding to r_c in section 5. If the ambient vapor pressure exceeds this value, no equilibrium condition is possible between the droplet and the environment, and it must continue to grow until conditions are altered. A rise in humidity, as indicated above, means that this maximum value will be exceeded for successively smaller and smaller nuclei. Since these smaller nuclei are present in increasingly larger numbers, the consumption of water increases until finally the humidity no longer rises, after which the consumption of water is generally slightly faster for a steady cooling rate than is needed to maintain a balance, and the humidity gradually falls, approaching saturation.

In this way the number of growing droplets is determined, the smaller droplets, passing this humidity "barrier", dominating the water consumption thereafter as $N \cdot (dm/dt)$ increases for these smaller sizes (see for example fig. 22). In other words the maximum humidity is determined by the nucleus (or drop size) distribution and the cooling rate. The drop size distribution is determined largely by the maximum humidity. Hence there is a combined effect of the vertical velocity and the nucleus distribution. These are the main variables therefore to be investigated here. The other factor in these computations which can influence the above factors is the falling velocity of the droplets. This has the effect of a continual change in the drop size distribution at one level until a steady state situation is obtained. At points where some particles have a fall velocity equal to the updraft, a very high concentration of particles can develop. If this point lies in the zone of maximum humidity it can affect not only the number of large droplets but also the number of small droplets by reducing the environmental humidity.

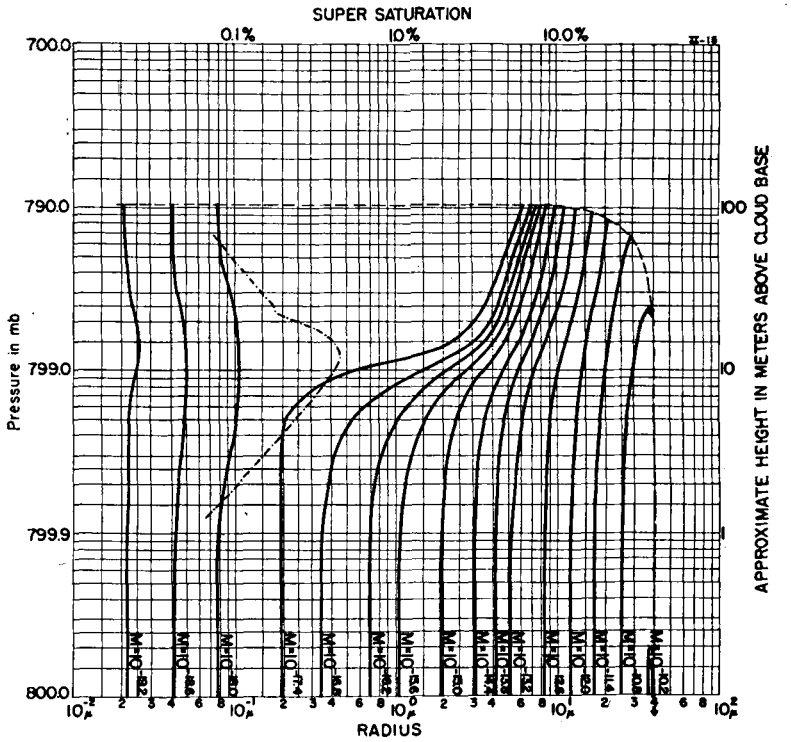

Fig. 10. Computation for a medium nucleus concentration, Distribution II at 15 cm /sec rate of rise. Data represented as in Fig. 9.

One further point is important to bear in mind. In two similar cloud droplet distributions, drops of the same radius may have formed on quite different nucleus sizes due to different initial nucleus distributions or environmental conditions. Measurements of droplet size and number in natural clouds therefore cannot determine to any fine degree the probable size of the nuclei involved during the formation of the cloud. It is possible for two quite similar cloud droplet spectra to have formed on different nucleus spectra due to higher supersaturation in one instance. Hence one is primarily concerned with comparing the cloud spectra produced and not the *radii* of the droplets formed on a *given nucleus size* in the different computations discussed below.

a) *The effect of the different nucleus spectra studied on the cloud droplet spectra*

In figures 9, 10 and 11 the results of three computations made for different nucleus distributions at approximately the same rate of rise (15—16 cm/sec) are shown. Sixteen nucleus size groups, representing the Distributions I, II and III, shown in figure 5, were used. In these three figures and in the similar figures which follow, the radii of the droplets formed on the different nucleus size groups are plotted against their height above cloud base (100 % humidity). Initial radii of the nuclei are the same in all cases. In the case of Distribution I, all but two of these sixteen nucleus sizes exceeded their critical radii and grew to cloud droplet size. In the case of Distributions II and III all but three grew. The minimum nucleus to grow was $M = 10^{-17.4}$ moles for Distributions II and III and $M = 10^{-18}$ moles for Distribution I. This represents nuclei which belong to the largest Aitken nucleus size groups.

The total number of growing drops in these three cases, however, is perhaps of somewhat greater interest. In the case of Distribution I approximately 1.3×10^7 growing drops were produced while for Distributions II and III only slightly more than this number, 4.7×10^7 were produced.

If we make the same comparison for a more rapid rate of rise, 100 cm/sec, as shown in figures 12, 13 and 14, we find that the drop

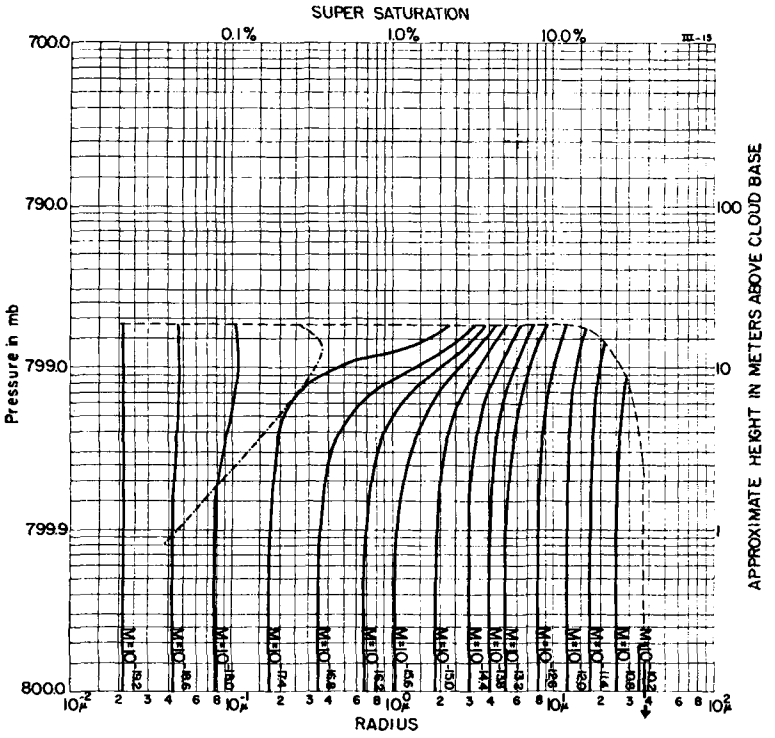

Fig. 11. Computation for dense nucleus concentration, Distribution III at 15 cm/sec. Data represented as in Fig. 9.

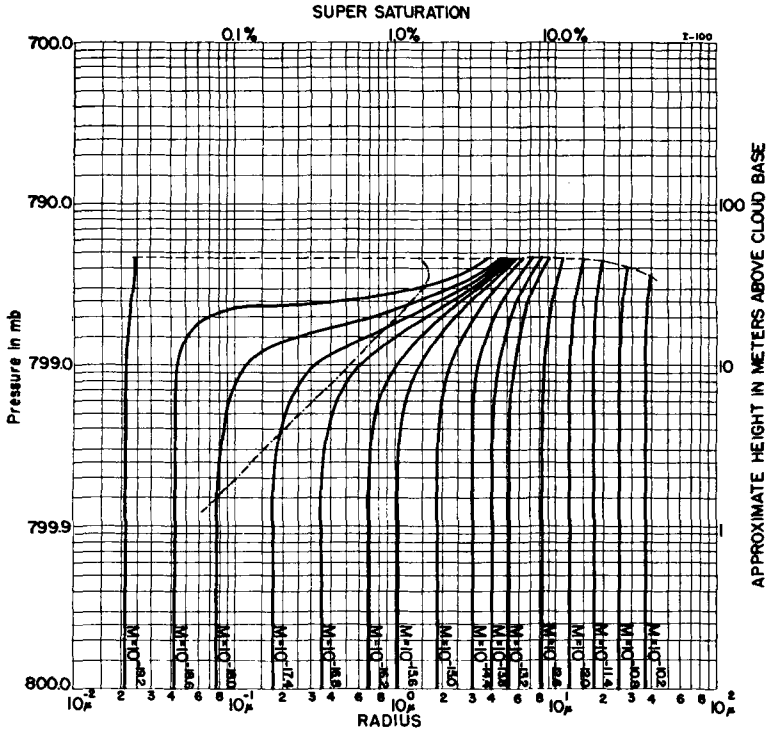

Fig. 12. Computation for sparse nucleus concentration, Distribution I at 100 cm/sec of rise. Data represented as in Fig. 9.

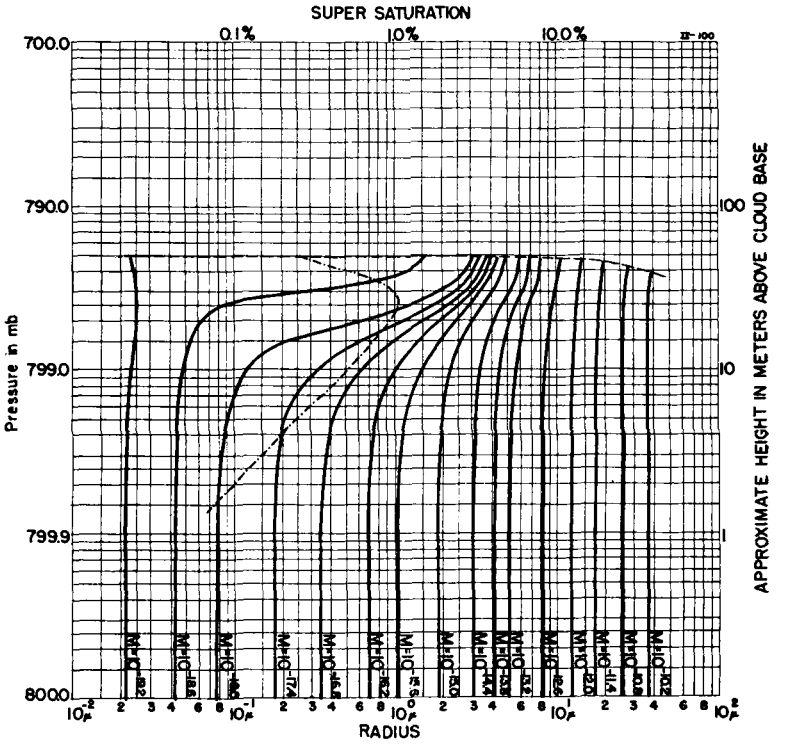

Fig. 13. Computation for medium nucleus concentration, Distribution II at 100 cm/sec rate of rise. Data represented as in Fig. 9.

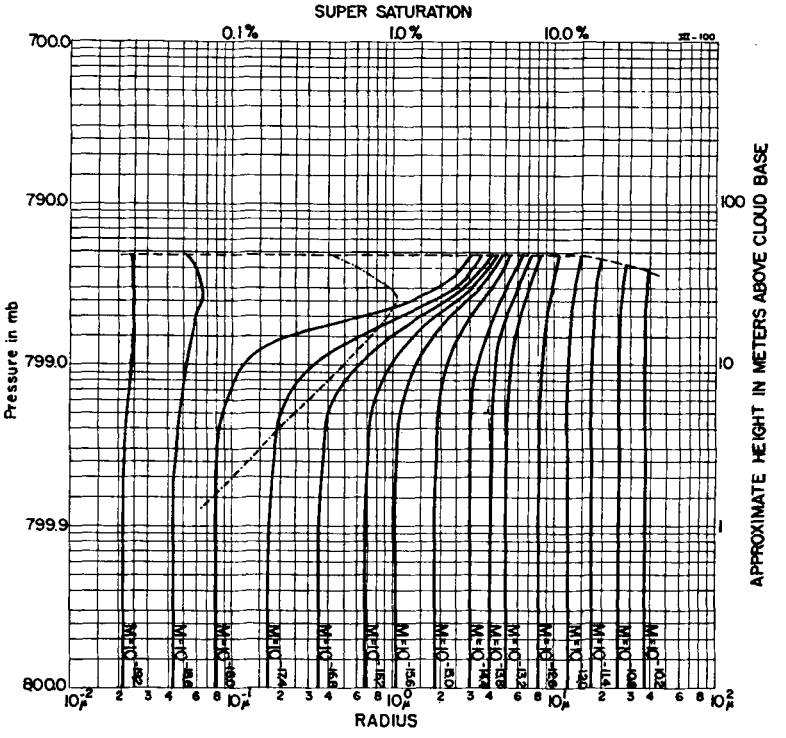

Fig. 14. Computation for dense nucleus concentration, Distribution III at 100 cm/sec rate of rise. Data represented as in Fig. 9.

numbers are altered much more dramatically. Here Distribution I produces 2.5×10^7 growing cloud droplets on nuclei down to $M = 10^{-18.6}$ in size. Distribution II produces however 4.7×10^8 or twenty times as many growing droplets on nuclei ranging down to the same size. In contrast Distribution III produces *fewer* growing droplets, 1.4×10^8, due to the fact that the growth of the larger number of large nuclei was sufficient to slightly lower the maximum supersaturation in this case.

It should be emphasized that due to the use of discrete size categories of nuclei both the maximum supersaturation and the number of cloud particles produced are accurate only within the limits marked out by two adjacent groups of nuclei. This is to say that the maximum supersaturation which would be reached if a continuous representation of the spectrum were used must lie between the critical supersaturation values representing the smallest two groups *to grow*, and the critical supersaturation value for the largest nucleus group, whose droplets *do not grow* past their critical radius. Consequently, the fact that slightly more growing droplets were produced for Distribution II as opposed to Distribution III in this latter case probably has less significance than it appears to have, since the maximum supersaturation reached in the two cases was so nearly the same, and the slight difference happened to be just sufficient to allow the next category to grow.

This behavior should be discussed in terms of theoretical factors which are related here. The problem is in the nearly balanced adjustment of the rate of water consumption to the rate of cooling. Two factors are involved, the number of cloud droplets and their rate of growth. The water consumption is:

$$\sum_{i=1}^{j} N_i \frac{dm_i}{dt}$$

m_i = mass of the droplet in group i

N_i = number of droplets in group i

j = number of actively growing groups

$N = \sum_{i=1}^{j} N_i$ = number of actively growing droplets

An increase in relative humidity can increase either N or $\frac{dm}{dt}$ = depending upon the nature of the distribution, and the rate of rise. If the rate of rise is extremely slow, the largest particles, in spite of their long time lag, can keep abreast of the cooling rate and consume all the water. As the rate of rise or cooling increases so does the humidity, hence starting new groups of droplets, with shorter time lags,

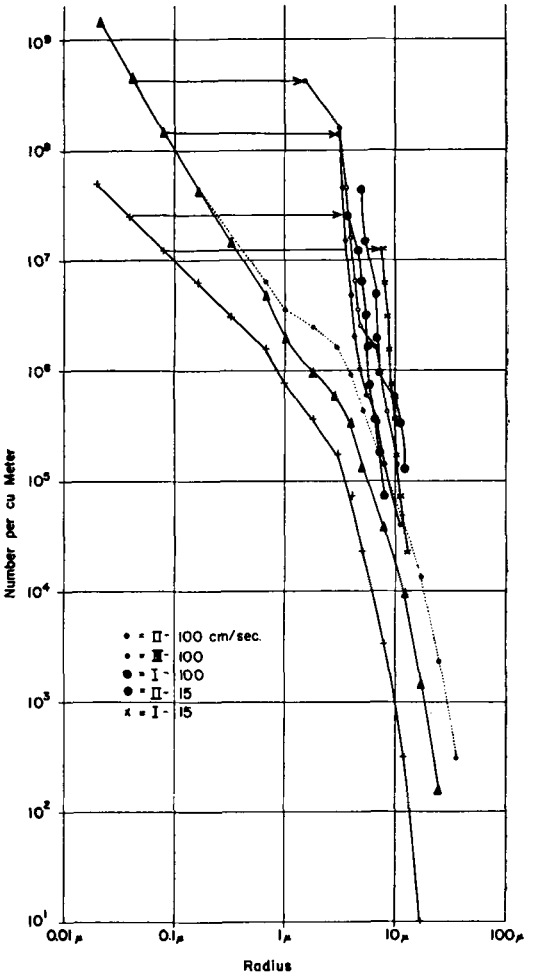

Fig. 15. A comparison of the cumulative number and radius of the droplets at 45 to 50 meters up into the cloud produced by the *three different distributions* at the *same rate of rise*. Distribution III at 15 cm/sec was computed only to 18 meters and therefore is not included. Initial radii and numbers are indicated by the curves at left side of diagram.

growing until the actively growing droplets can limit the further increase in relative humidity. This is to say that as the vertical velocity is increased the water consumption is first adjusted mainly by changes in N but with further increases the final adjustment is increasingly in terms of $\frac{dm}{dt}$ because for very small nuclei, the critical values of the supersaturation rises rapidly with decreasing r_c (see section 5). In the "dense" distribution N is the variable which is controlling. In the "sparse" distribution the adjustment takes place only when $\frac{dm}{dt}$ is large.

Therefore in the cases cited above, at a slow rate of rise (15 cm/sec), N adjusted to nearly the same value for the three distributions, while at 100 cm rate of rise the term $\frac{dm}{dt}$ became more important in the Distribution I case than for Distributions II and III. To the degree that these distributions are characteristic of natural conditions one may conclude that initial differences in nuclei distributions are more manifest in cloud droplet concentrations when the vertical velocity is greater.

Another way of approaching this conclusion is to consider the *slope* of the nucleus distribution curves. "Dense" nucleus distribution as used here refers of course to a larger number of large, "Woodcock" nuclei while the "medium" concentration has the same number of smaller nuclei but fewer Woodcock nuclei.

Distribution I ("sparse") however has fewer nuclei in all categories. These distributions were chosen to represent *observed* conditions and hence do not clearly demonstrate the implied differences in cloud droplet concentration which may result from the two variables, *distribution slope* and *concentration*.

Given otherwise equal conditions a steep distribution slope will prevent the supersaturation from increasing to a large value since the *number* of growing cloud droplets adjusts more rapidly to increasing humidity

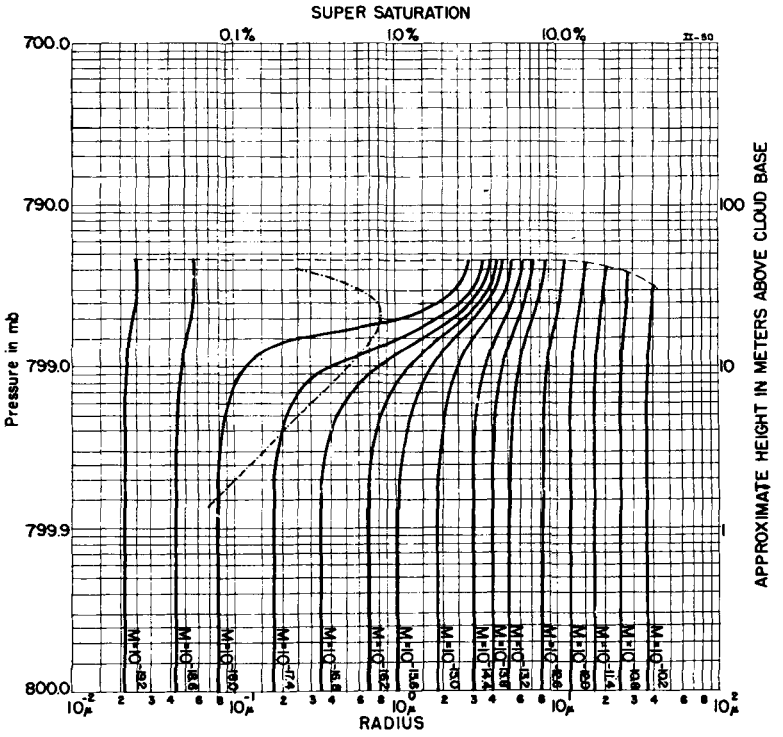

Fig. 16. Computation for medium nucleus concentration, Distribution II at 50 cm/sec rate of rise. Data represented as in Fig. 9.

conditions. If the slope is more gradual there is more interaction between the growth rates of the large and small droplets in the spectrum. Here much greater increases in humidity are required to start new groups of nuclei growing unstably and these increases of humidity become increasingly retarded by greater water consumption by the larger cloud droplets produced by the same higher humidity conditions.

In the cases discussed above, the points which divide the nucleus spectrum from the cloud droplet spectrum lie in the range $M = 10^{-18.6}$ to $M = 10^{-17.6}$ In these points Distributions II and III have the same slope and almost the same number while Distribution I has a more gradual slope and a smaller concentration.

The larger difference in number of growing droplets between Distribution I and Distribution II at the rapid rate of rise seems to indicate that the important fact in this discussion is the *slope* of the distribution curve in the range of the smallest few categories of nuclei to grow. An increase in vertical velocity produces a greater change in the number of cloud droplets formed on high slope distributions than for the opposite.

These results are combined for comparison in figure 15. Here the drop size spectra produced at 45 to 50 meters above cloud base are compared for five of the six cases cited above. The case for Distribution III at 15 cm/sec was computed only to about 12 meters above cloud base and consequently is not included. In this diagram both the number and the radii of the droplets are represented as they might be if measured in natural cloud. In addition to the number comparison made above, it is possible here to compare the differences in radii which result from the different conditions represented. In all cases the droplets formed on nuclei with initial radii smaller than 3 μ have nearly equal radii at distances more than a few tens of meters above cloud base. Droplets formed on larger nuclei due to their longer time constants (see sec. 5) continue to exhibit their initial size differences for much longer growth intervals. Consequently the radii differences at the large end reflect mainly the differences in the original nucleus spectrum.

b) *Some additional effects of varying vertical velocity on cloud droplet spectra*

It is also instructive to note differences in drop number and size which result from variation in the rate of cooling or vertical velocity alone. One such comparison is possible with Distribution II by referring to figures 10, 13 and 16 which show the growth of the Distribution II particles at 15, 50 and 100 cm/sec. Each increase of the vertical velocity increases

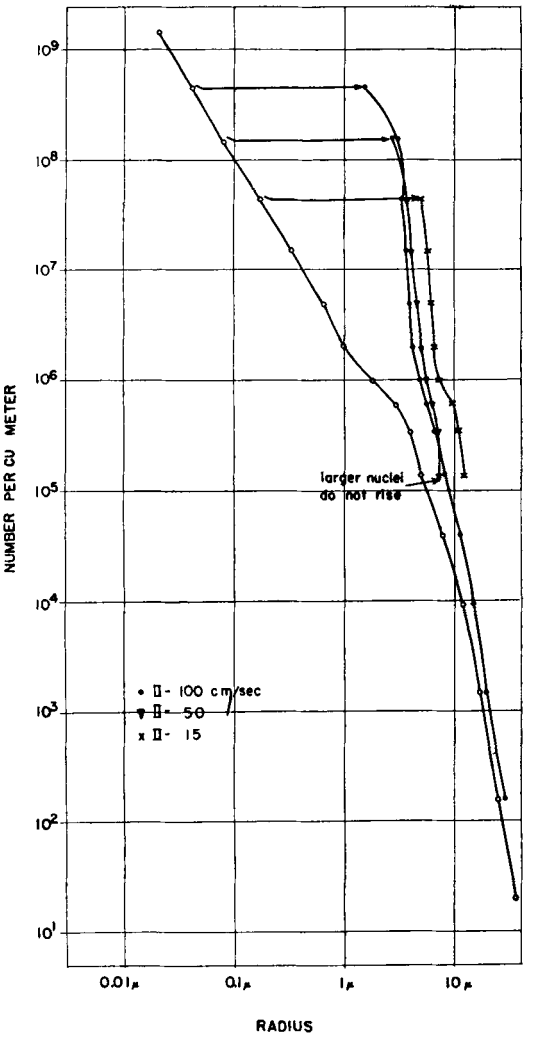

Fig. 17. A comparison of the number and radius of the droplets at 45 to 50 meters above cloud base produced by three different rates of rise (15, 50, 100 cm/sec) on the medium nucleus concentration, Distribution II. Original distribution is at left marked with open circles.

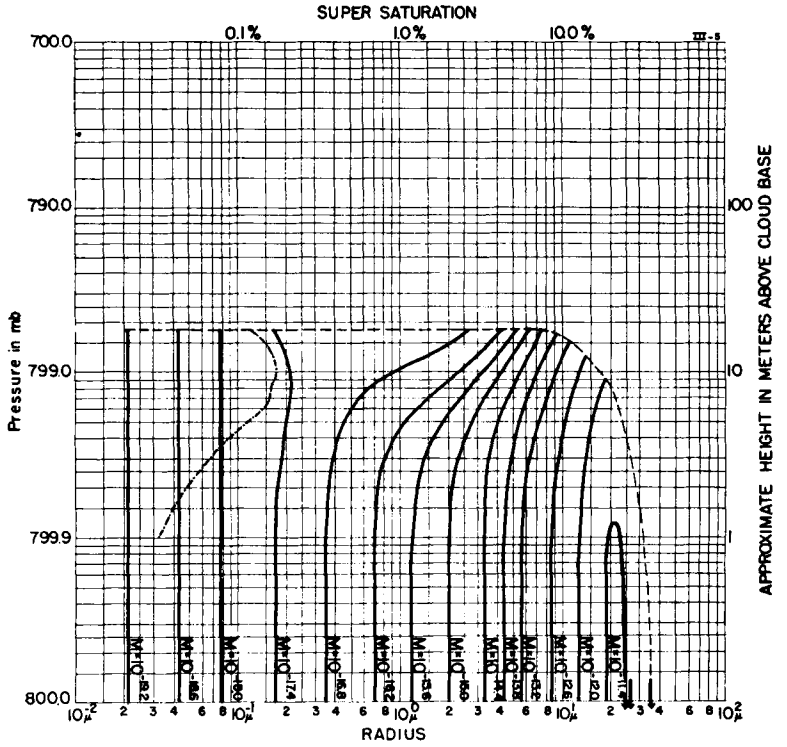

Fig. 18. Computation for a dense nucleus population. Distribution III at 5 cm/sec rate of rise. Data represented as in Fig. 9.

the number of growing particles roughly by a factor three, by including among the growing droplets one more smaller group of nuclei. This is to say that for 15 cm/sec there were 4.7×10^7 growing droplets, while at 50 cm/sec there were 1.4×10^8, and at 100 cm/sec there were 4.7×10^8 droplets. This is nearly as great a variation in number as the different distributions produced at 100 cm/sec rate of rise, that is, ten times as opposed to thirty.

In fig. 17, the cumulative cloud droplet distributions produced at 45 to 50 meters above cloud base are compared both by radius and number, as they were in figure 15. In the case of the slowest rate of rise both the minimum growing drop size and the maximum size of the droplets are larger, a condition which is believed by most investigators to be conducive to the coalescence process.

Note in figure 17 (and in figure 15) that it would be very difficult if not impossible to distinguish these drop size distributions from one another by measurements in natural conditions in terms of the size of the droplets produced. The smaller droplets are so nearly the same size that the inaccuracy of measurements and local variations in cloud would completely mask these size differences. At the large end of the spectrum the possibility of coalescence between the droplets rules out the possibility of detecting differences between the different drop size spectra produced. Only the *number* of cloud droplets is indicative of the conditions in which the droplet spectrum first forms.

c) *Comparison of the extreme cases in the computations*

It might be thought that a *rapid rate* of rise for a *sparse* nucleus population and a slow rate of rise for a dense concentration should provide the greatest contrast in the resulting condensation cloud spectra. In the first of these cases the supersaturation should rise to its highest possible value while the number of cloud particles would be limited by the nucleus

spectrum. This should produce a more uniform spectrum since the condensed water would be "forced" onto a smaller number of nuclei. The largest nuclei, due to their longer time constants, also lag behind more in the case of rapid cooling which further tends to narrow the size spectrum.

In the case of a slow rise on a dense population, the size of the smallest droplets to grow is not much larger than for the sparse distribution, while the slower cooling rate permits more of the larger nuclei to "keep up" with the condensation rate. In this way a broader spectrum should be formed.

With these suggestions in mind it is interesting to look at two such cases as computed here. The two extreme cases computed were the case of Distribution I at 100 cm/sec shown in fig. 12 and Distribution III at 5 cm/sec shown in fig. 18. In these cases the number of growing cloud droplets produced was nearly the same (2×10^7 vs. 1.5×10^7) but the radii were quite different. However, at some few 100's of meters above cloud base it is clear that the dominant size group (smallest) will have essentially the same radius in both instances and only the larger particles will differ markedly.

These computations were not carried out to the same height above cloud base and strict comparison at the same height cannot be made. By recourse to the type of graph used in figures 15 and 17 though, it is possible to extrapolate visually the cloud droplet spectrum. The smaller end becomes more and more uniform in size, as the two cases plotted in fig. 19 show. Here it is clearly seen how the size spectra diverge rapidly toward larger particle sizes. This is true even though the slower rate of rise used in the Distribution III case had not carried the particles nearly so high into the cloud when the computation was stopped as in the case of the rapidly rising Distribution I case. However, there is one limiting or compensating effect to offset this tendency. This is the fact that if the rate of rise is slow, the largest particles begin to settle out against the rising current, tending to narrow the spectrum from the large end.

Actually the largest differences in droplet spectra in these computations seem to come in terms of droplet number or *concentration*. These differences occurred for quite the opposite pairs

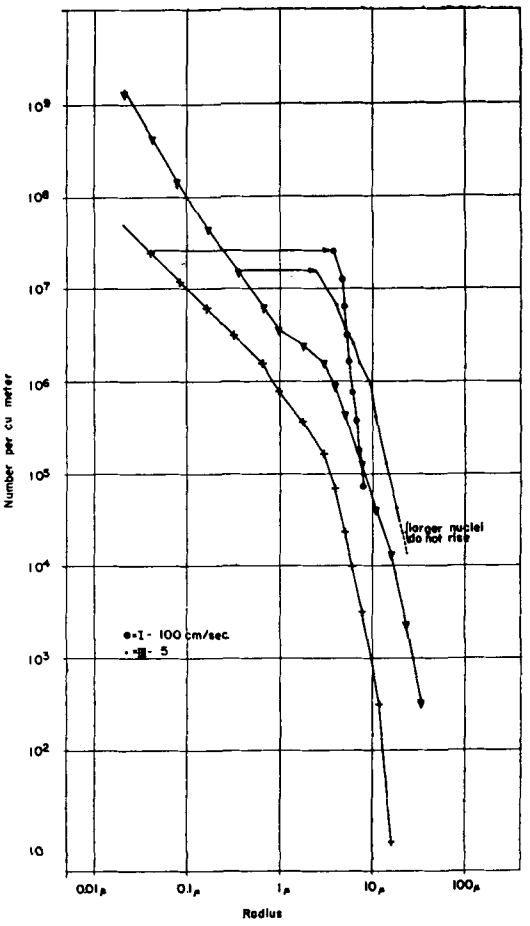

Fig. 19. Cumulative drop size distributions resulting from two extreme cases in the computations, sparse (Dist I) concentration at 100 cm/sec rate of rise and dense (Dist III) at 5 cm/sec producing more and less uniform spectra respectively.

of conditions from those discussed above, namely between a sparse population with a slow rate of rise and a dense population with a rapid rate of rise. These conditions are represented here by the 15 cm/sec rate of rise for the Distribution I case and 100 cm/sec for the Distribution II (or III) case, shown in figures 9 and 13. The fact that this extreme difference occurred for the medium rather than the most dense population of particles has been discussed above in section 7a. If a somewhat more rapid rate of rise had been chosen, the denser population of Distribution III would have produced more growing drop-

lets than Distribution II. Consequently this fact is only of minor importance.

In the two cases represented here there is a difference of thirty times in the number of particles per unit volume of cloud. This *range of particle concentration* is in agreement with cloud droplet measurements made by a number of the most recent investigators, ZAITSEV (1950), WEICKMANN and AUFM KAMPE (1953), SQUIRES (1957, 1958) etc. Except for the smallest droplets, droplet radii *all along the spectrum* in almost all cases are smaller than those observed in clouds.

d) *Deviations from the moist adiabatic lapse rate*

It is possible also to look at the total amount of water condensed at various levels above cloud base as indicated in the computations and compare it with the amount theoretically condensed according to moist adiabatic expansion. Such a comparison here is not *strictly* accurate due to the approximation used for the dry adiabatic lapse rate. Deviations due to this discrepancy however are small since the vertical distances considered are all less than 80 meters.

Such a comparison is possible by considering the curves shown in figure 20. In this figure the dashed line indicates the water which would have been condensed if the process were moist adiabatic while the curves at the left indicate the water condensed at each level for the Distribution II cases at 15, 50, and 100 cm/sec. The curves are separated until air reaches from 30 to 50 meters above cloud base while after this, condensation proceeds almost exactly along the moist adiabatic condensation line.

In figure 21 the values computed for the different distributions are compared at 15 and 100 cm/sec. The largest deviation from the moist adiabatic rate is indicated for the Distribution I case at 100 cm/sec where, unfortunately the computation was stopped before the condensation rate approached the moist adiabatic condensation line. Extrapolation of this curve however indicates that the curves join at about 80 meters.

Differences between the curves for the three distributions at 15 cm/sec are of little interest while it appears that sparse distributions at higher vertical velocities might cause deviations from the moist adiabatic lapse rate up to 100 meters or more. Such deviations could be detected in carefully taken cloud temperature measurements and suggest the possibility of roughly identifying nuclei conditions in this way.

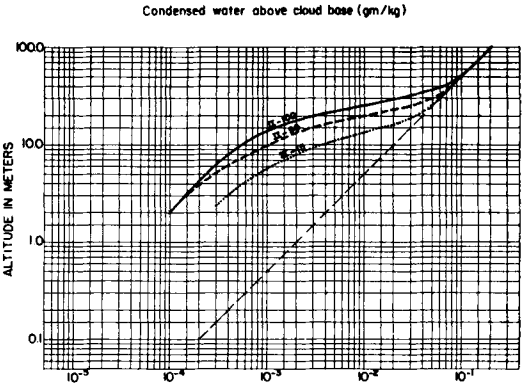

Fig. 20. Deviations of the cloud liquid water content *comparing different rates of rise* from that computed with the moist adiabatic assumption. The straight line indicates the cloud liquid water with moist adiabatic assumption. The curved lines show the liquid water as computed for the three different rates of ascent for Distribution II.

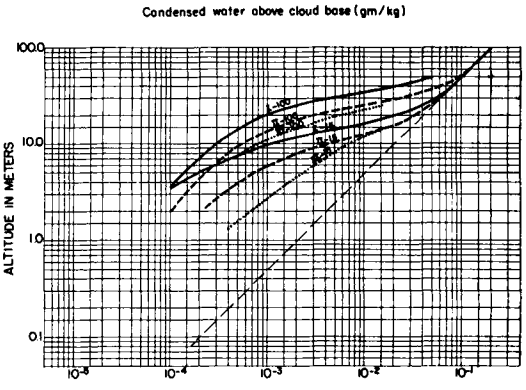

Fig. 21. Deviations of cloud liquid water from that computed with moist adiabatic assumption *comparing the different distributions* at two rates of rise. The curved lines show the cloud liquid water as computed in this study while the straight line indicates that computed with the adiabatic assumption.

8. Discussion

It has long been recognized that condensation alone cannot account for the range of cloud and rain droplet sizes which are found in nature. In spite of this fact it must be recognized that the condensation process provides

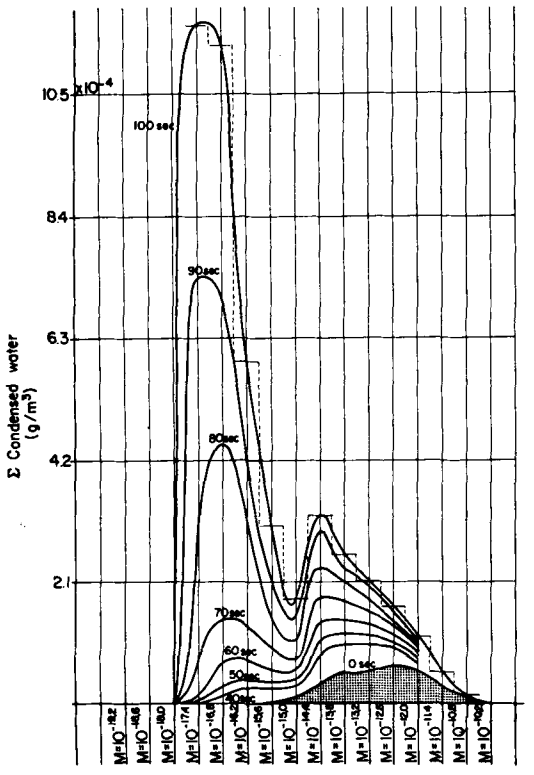

Fig. 22. Graph indicates the liquid water condensed on the different nuclei sizes in Distribution II at 15 cm/sec rate of rise at given time intervals after the beginning of the computations. It shows how the large nuclei consume nearly as much water up to level of maximum supersaturation (13 meters) as the smaller ones, but soon thereafter nearly all water is condensed on the smallest few nuclei size.

the first spectrum of cloud droplets which other processes later modify and determines the *maximum concentration* of cloud particles. Because of this, any theoretical discussion of other processes, such as coalescence, drop breaking, entrainment, turbulence, freezing etc., which alter the condensation produced spectrum, should be based on as complete an understanding of this process as possible.

From the present computations several general features of the condensation process can be seen rather well. If the water which is condensed on the different sized droplets is graphed, as in figure 22 above, it is possible to get a visual impression of the dynamics of the condensation process. In this diagram we can visualize the building up of liquid water on the Distribution II nucleus spectrum during the early stages of condensation. It can be seen that, as postulated above, the largest part of the condensed water initially goes to the largest nuclei. Gradually as the humidity continues to rise the liquid water condensed on the smaller nuclei increases until after 70 seconds the smaller droplets contain about the same total amount of water as the larger ones. Shortly thereafter, in an almost explosive way, the smallest droplets grow until they contain nearly all the cloud water.

In terms of the theoretical remarks in section 3, the initial dominance of the larger particles is due to the fact that these particles have a higher salt concentration and a larger initial radius, hence the vapor pressure lowering over the droplet is very great and the water content of the individual droplet is increased rapidly. This condition prevails for these droplets for a very long time but they are too few to play a dominant role for long as they do not consume water at a rate sufficient to keep the humidity from rising. They can, however, if sufficiently numerous, reduce the maximum humidity somewhat and thereby reduce the total drop number. Gradually then the smaller and smaller droplets begin to grow, each group consuming more water than the next larger group until the humidity no longer rises.

In fig. 22 therefore the double maximum is due to the fact that the droplets at the large end of the spectrum are growing by virtue of their *hygroscopicity*, which in some cases produces more than 1 % vapor pressure difference between the drop surface and the environment, while the smaller droplets are growing largely due to the increased humidity of the *environment*.

The effect of the different distributions of particles is illustrated by comparing fig. 22 with fig. 23 where the same type of graph is shown for Distribution III at the same rate of rise. Here the greater number of large particles increases the liquid water content in the large end of the spectrum so that for the first 100 seconds, as opposed to 70 seconds for Distribution II, it dominates the growth. This is noteworthy since the maximum humidity (see figures 10 and 11) is reached at 12 to 13 meters in both instances, illustrating how these large particles can in some instances

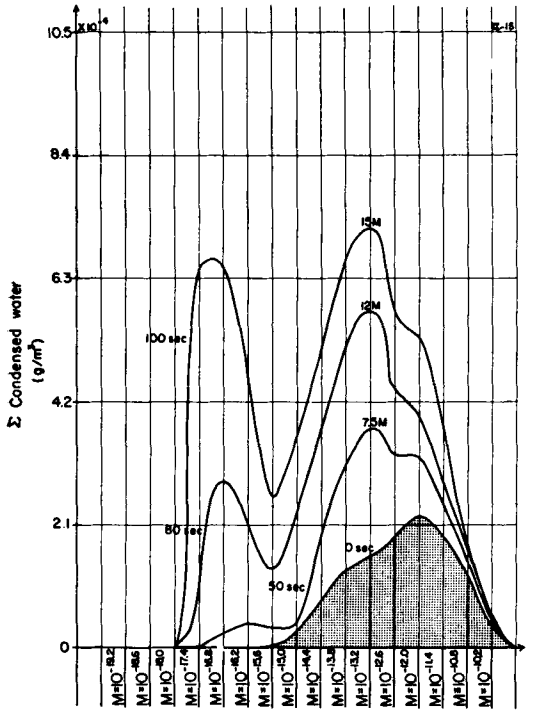

Fig. 23. Same as fig. 20 for Distribution III at 15 cm/sec showing greater effect of the largest nuclei.

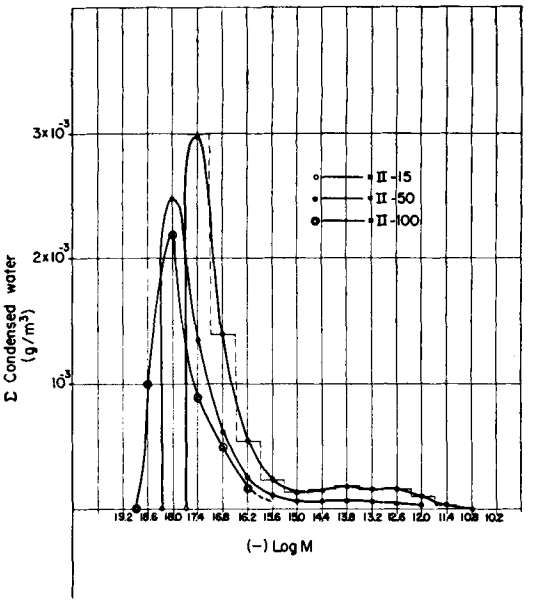

Fig. 24. Graph shows the liquid water contained in the droplets formed on the different nuclei sizes in the Distribution II case. 45—50 meters above cloud base (100 % R.H.) at 15.50, and 100 cm/sec rates of rise.

limit the maximum humidity and hence the droplet concentration.

After a period of time sufficient to carry the particles 45 to 50 meters high, nearly all cloud water is contained in the droplets formed on the smallest two or three nucleus sizes. This is shown in figures 24 and 25 which are similar to figures 22 and 23 except that the vertical scale has been shortened and the comparisons are made for 45—50 meters above cloud base. In figure 24 the effects of the three rates of rise on the Distribution II cases are compared. In fig. 25 the three distributions are compared at the same rate of rise, 100 cm/sec.

9. Summary

a) The *number* of cloud particles produced is dependent *both* on the vertical velocity and the nucleus distribution. This result is at variance with Howell's conclusion that the vertical velocity was the primary factor, and is mainly a result of the differences in the

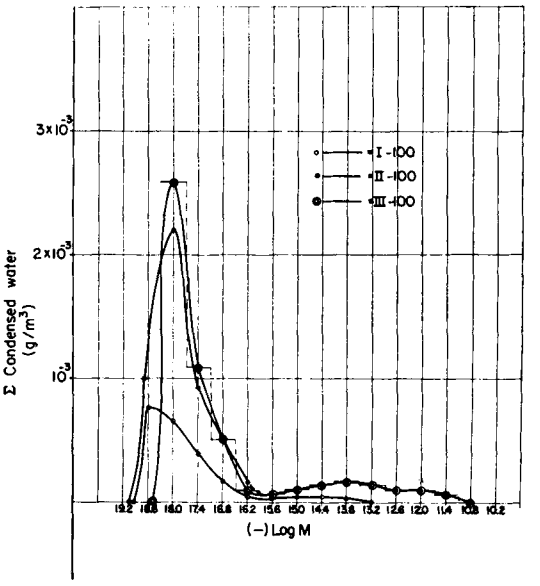

Fig. 25. Liquid water contained in the droplets formed on the different nuclei sizes of the three Distributions I, II, and III at 10 cm rate of rise 45—50 meters above cloud base.

nucleus spectra considered. The cloud particle concentrations calculated agrees with the observed range in natural clouds.

b) The *radii* of droplets found at given heights above cloud base, both by reason of differences in concentration and growth rate, may be significantly different in the different conditions studied here. Although in general, if given enough time, all growing droplets converge toward a uniform radius, the rate at which this takes place may be quite different. This is increasingly noticable as larger nuclei are considered. Presumably subsequent coalescence depends on these size differences and hence the conditions which produce them deserve considered attention.

c) The effect of drop sedimentation on condensation conditions is of importance

1) only when the vertical velocity is extremely slow (1 to 10 cm sec^{-1}),

2) there is an extremely dense nucleus distribution (such as Distribution III),

3) if there is an increase of settling droplets due to coalescence.

d) The drop size spectra indicated by these computations does not adequately describe the observed spectra in natural clouds. There are too few large droplets in the computed cases. The size and number of the smallest droplets however are in accord with observations.

e) The *relative* humidity values seldom exceed saturation by more than 1 % confirming Howell's conclusion. The depth of the layer where the lapse rate of temperature differs from the moist adiabatic may exceed 100 meters in some conditions of low nucleus concentrations.

Acknowledgement

The author is deeply indebted to Mr. Claes Rooth, Institute of Meteorology, University of Stockholm, for considerable assistance in the preparation of this study for the Besk Computer, for aid in determining the stability of the computations, and along with other members of the International Meteorological Institute for many stimulating and helpful discussions.

REFERENCES

ALTY, T. and MACKAY, C. A., 1935: The accommodation coefficient and the evaporation coefficient of water. *Proc. Roy. Soc.*, London, **A 199**, pp. 104—116.

ARONS, A. B. and KIENTZLER, C. F., 1954: Vapor pressure of sea-salt solutions. *Trans. A. G. U.* **35**, pp. 722—728.

BERGERON, T., 1935: On the physics of cloud and precipitation. *Proc. 5th assembly UGGI*, Lisbon **2**, pp. 156—178.

ERIKSSON, E., 1952: Composition of atmospheric precipitation. *Tellus* **4**, pp. 215—232.

ERIKSSON, E., 1952: Composition of atmospheric precipitation. *Tellus* **4**, pp. 280—303.

FRÖSSLING, N., 1938: *Beitr. Geophys.* **52**, p. 170.

GUNN, R. and KINZER, G. D., 1949: The terminal velocity of fall for water droplets in stagnant air. *J. of Met.* **6**, pp. 243—248.

HOUGHTON, H. G., 1938: *Bull. Amer. Met. Soc.* **19**, p. 152.

HOWELL, W. E., 1949: The growth of cloud drops in uniformly cooled air. *J. of Met.* **6**, pp. 134—149.

JOHNSON, J. C., 1954: Physical Meteorology. *John Wiley and Sons*, New York, 210 pp.

JUNGE, C., 1952: *Ber. Dtsch. Wetterdienst US Zone*, **35**, p. 261.

KEITH, C. H. and ARONS, A. B., 1954: The growth of sea-salt particles by condensation of atmospheric water vapor. *J. of Met.* **11**, pp. 173—184.

KÖHLER, H., 1921: Zur Kondensation des Wasserdampfe in der Atmosphäre. *Geophys. Publ.* **2**, pp. 3—15.

— 1926: Zur Thermodynamik der Kondensation an hygroskopischen Kernen und Bemerkungen über das Zusammenfliessen der Tropfen. *Medd. Met. Hydr. Anst. Stockholm* **3**:8.

— 1936: *Trans. Faraday Soc.* **32**, p. 1152.

— 1941: *Reg. Soc. Sci.* Uppsala, *Nova Acta*, **12**.

— 1950: On the problem of condensation in the atmosphere. *Medd.* **15**, *Nova Acta Reg. Soc. Sci. Ups.*, Uppsala, 75 pp.

LANGMUIR, I., 1944: Super cooled droplets in rising of cold saturated air. *General Electric Company*, Schenectady, N.Y., 150 pp.

MCDONALD, J. E., 1953: Erroneous cloud-physics applications of Raoult's law. *J. of Met.* **10**, pp. 68—70.

MASON, B. J., 1957: The physics of clouds. *Oxford Press*, 470 pp.

— and GHOSCH, D. K., 1957: The formation of large droplets in small cumulus. *Quart. J. Roy. Met. Soc.* **83**, pp. 501—507.

MOORE, D. J. and MASON, B. J., 1952: *Quart. J. Roy. Met. Soc.* **78**, p. 596.

MORDY, W. A., 1953: A note on the chemical composition of rainwater. *Tellus* **5**, pp. 470—474.

PROJECT SHOWER 1957: Tellus 9, pp. 471—590.

ROOTH, C., 1957: On a special aspect of the condensation process and its importance in the treatment of cloud particle growth. *Tellus* **9**, pp. 372—377.

SQUIRES, P., 1952: The growth of cloud drops by condensation. I. General characteristics. *Austr. J. of Sci. Res.* **5**, pp. 59—86.

— 1952: The growth of cloud drops by condensation. II. The formation of large cloud drops. *Austr. J. of Sci. Res.* **5**, pp. 473—499.

— and WARNER, J., 1957: Some measurements in the orographic cloud of the Island of Hawaii and in trade wind cumuli. *Tellus* **9**, pp. 475—494.

SQUIRES, P., 1958: The microstructure and colloidal stability of warm clouds. *Tellus* **10**, pp. 256—271.

SVERDRUP, H. U. et al., 1942: The oceans. *Prentice-Hall*, p. 51.

VIERHOUT, R. R., 1949: On the formation of drops in clouds and fog. *Mededelingen en verhandelingen van het Koninklijk Nederlands Meteorologisch Instituut, De Bilt*, **125**, serie B, 20 pp.

WEICKMANN, H. K. and AUFM KAMPE, H. J., 1953: Physical properties of cumulus clouds. *J. of Met.* **10**, pp. 204—211.

WOODCOCK, A. H. and GIFFORD, M. M., 1949: Sampling atmospheric sea-salt nuclei over the ocean. *J. of Marine Res.* **8**, pp. 177—197.

WOODCOCK, A. H., 1953: Salt nuclei in marine air as a function of altitude and wind force. *J. of Met.* **5**, pp. 362—371.

— and MORDY, W. A., 1955: Salt nuclei, wind and daily rainfall in Hawaii. *Tellus* **7**, pp. 291—300.

ZAITSEV, V. A., 1950: Liquid water content and distribution of drops in cumulus clouds. *Trudy Glavnoi Geofizicheskoi Observatorii*, **19** Translation: *National Research Council of Canada, Tech. Trans.* **TT-395**, 21 pp.